Low-background technique and physics at BNO INR RAS

Vladimir Kazalov

Baksan Neutrino Observatory INR RAS

vvk1982@mail.ru
kazalov@inr.ru

7th International Conference on Particle Physics and Astrophysics,
Moscow, MEPhI, 2024

BNO INR RAS location:
vicinity of Mount Elbrus,
in the Baksan valley of Kabardino-Balkaria (Russia).

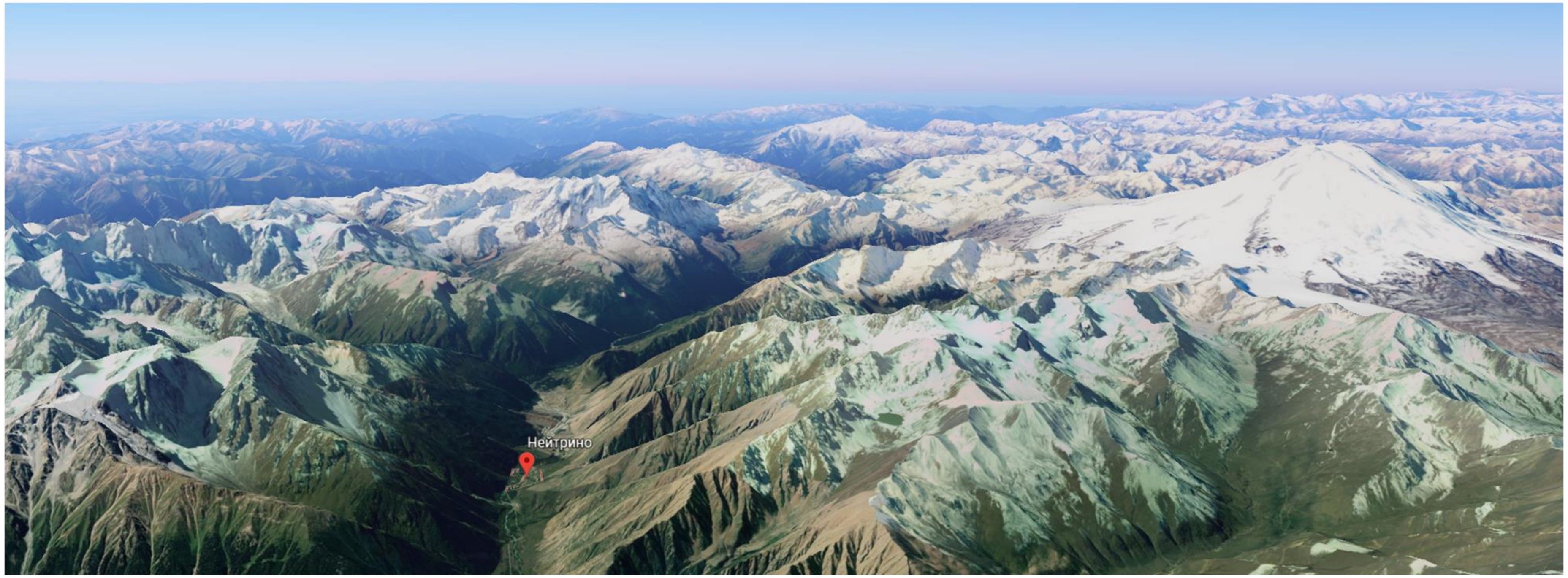

One of the areas of research is geophysics

Monitoring of the regional geodynamics of the Elbrus region in order to assess the risks of possible natural disasters.

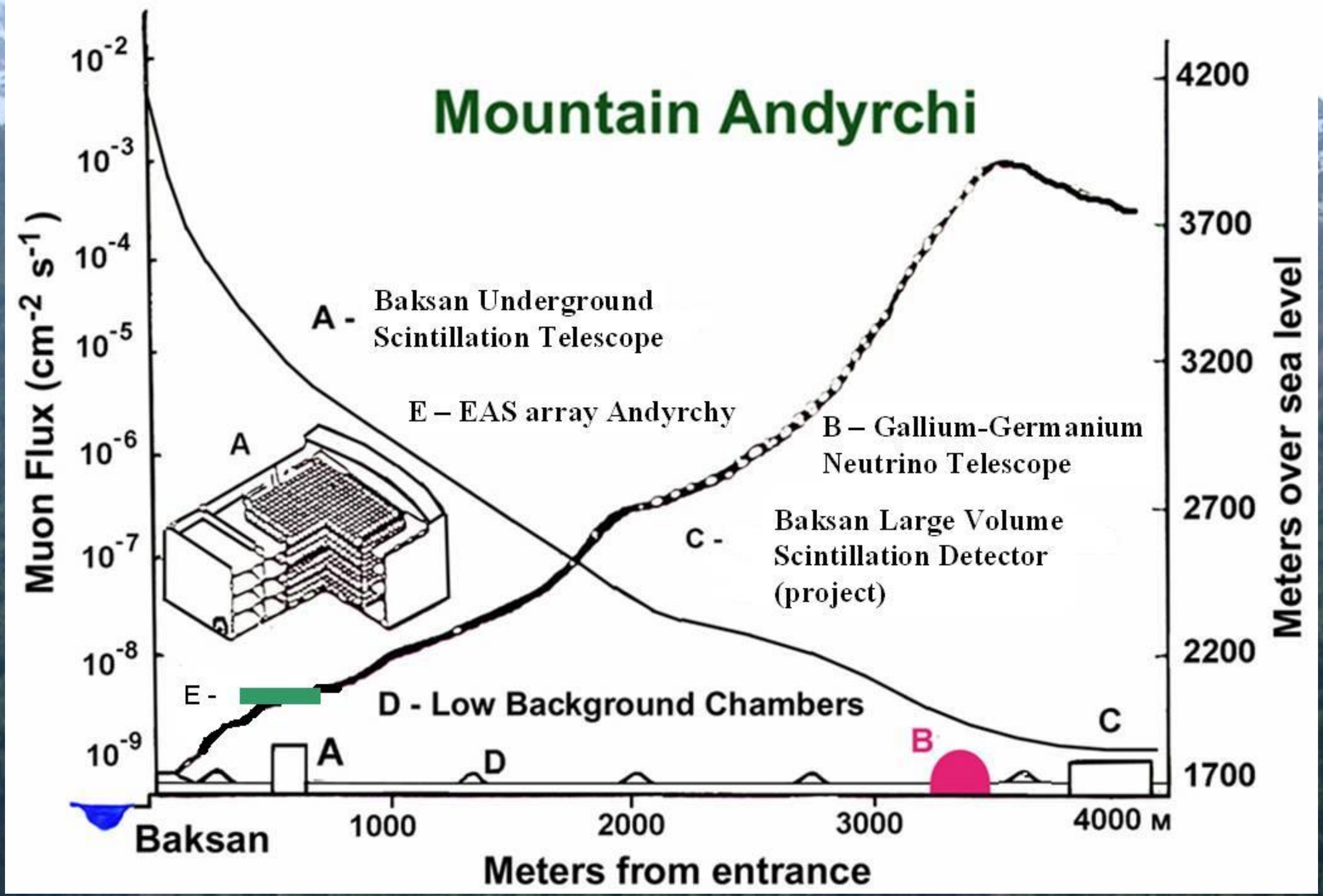

~ 1 muon/(m^2·10 h)
Large suppression of the cosmic rays background

Underground Laboratories of the BNO INR RAS

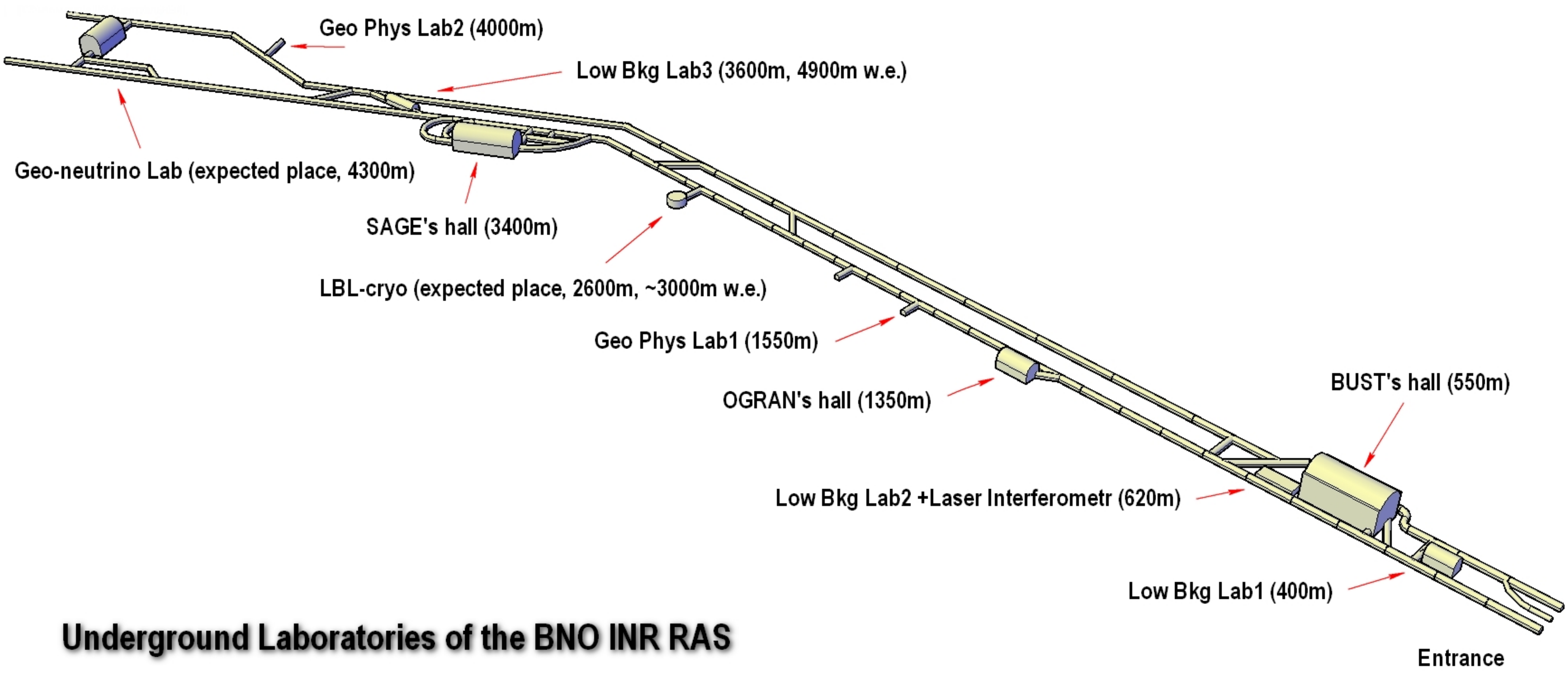

Low-background concrete at GGNT laboratory

- **Low-radioactive concrete is a key and unique feature of GGNT underground lab**: it serves as radiation shielding and structural reinforcement of rocks (at such a depth it is a prerequisite).
- Total volume of low background concrete is 2200 m^3, the thickness is 70 cm, total weight of frameworks made of steel siding is 370 t.
- Neutron flux is $3{,}8 \cdot 10^{-6}$ neutrons/cm^2/sec
- Gamma flux (0,2 – 3,2 MeV) is 15÷16 times less compare with the standard rock

Sketch of GGNT laboratory (scale 1:1000)

Main hall of 7 200 m^3 lined with 70 cm of low background concrete
Overburden: 2000 m (4.8 km w.e.)
Radon: 40 Bq/m^3
F_n (>1 MeV) = 1.4×10^{-3} $m^{-2}s^{-1}$
F_n (>3 MeV) = $6.28 \pm 2.2 \times 10^{-4}$ $m^{-2}s^{-1}$

1- Chamber of firefighting materials and equipment
2- Chamber of a car U-turn
3- Chamber of electric substation
4- Chamber of Air conditioning
5- Reload chamber
6- Main hall
7- Chamber of technical equipment
8- Chamber of exhaust ventilation
- Emergency chamber (10 persons x 2 weeks)

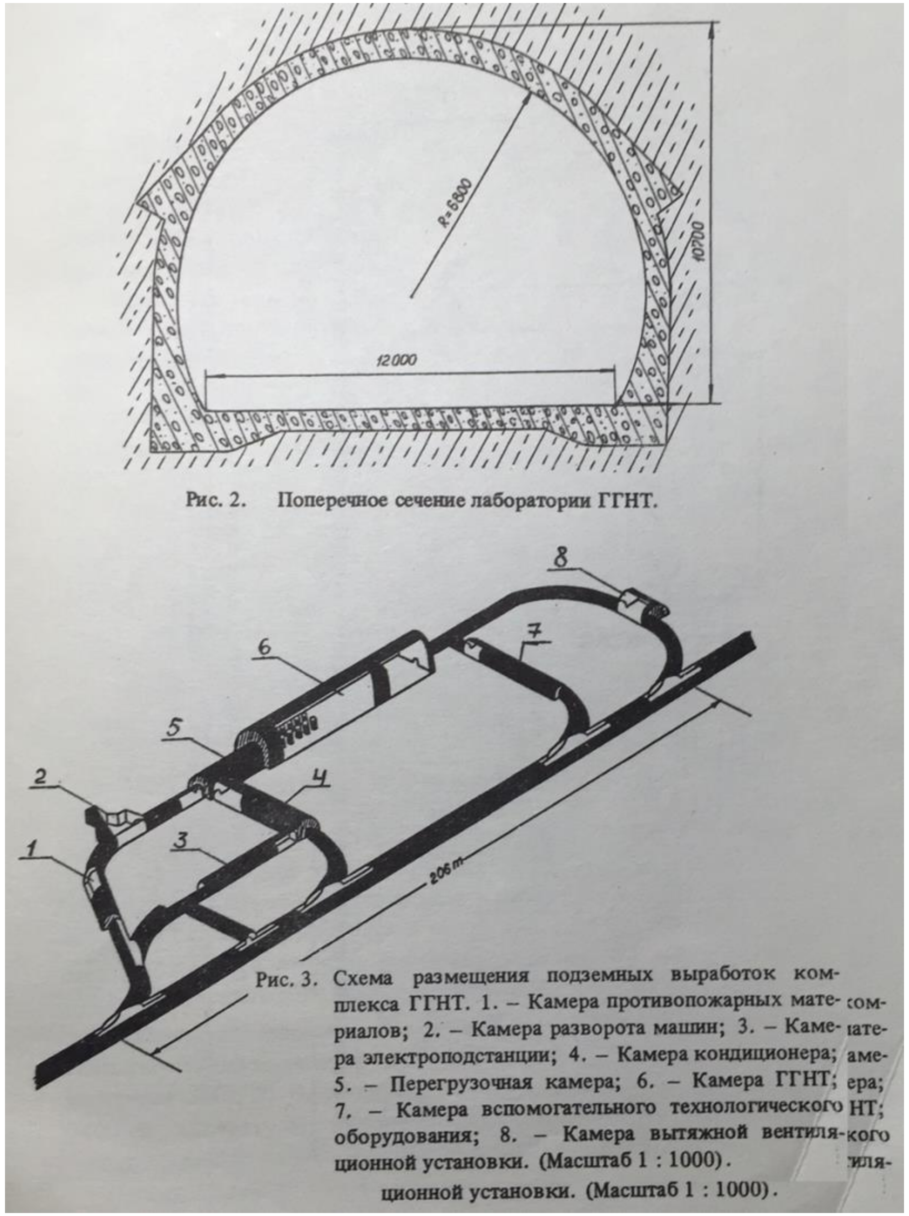

General view of GGNT laboratory - 2

- *Depth – 4700 m.w.e* $((3.03\pm0.10)\cdot10^{-9}\ \mu\ cm^{-2}\cdot s^{-1})$
- *Size – 60m×10m×12m*

Ga solar neutrino measurements

$\nu_e + {}^{71}Ga \rightarrow {}^{71}Ge + e^-$

Threshold 233 keV,
$T_{1/2}$ of ${}^{71}Ge$ = 11.43 d
${}^{71}Ga$: 40% in natural Ga

50 t of Ga = $1.7 \cdot 10^{29}$ atoms of ${}^{71}Ga$
Capture rate on Ga (SSM)~130 SNU
– 1.9 captures/day
– 26 atoms of ${}^{71}Ge$/month

Efficiencies: (extraction, chemical, counting) ~50%,
one run – ≈13 decays of ${}^{71}Ge$ atoms
Counting time of each run ~ 150 days

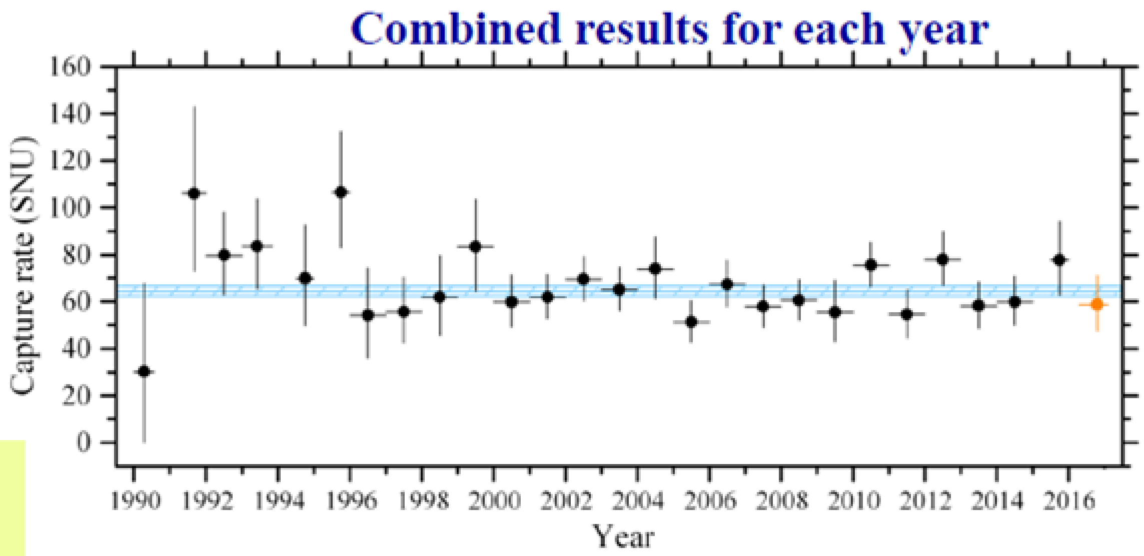

$$\text{Result}: 64.7 \pm 2.4(\text{stat.})\ {}^{+2.6}_{-2.8}\ (\text{syst.})\ SNU$$

$$\downarrow\ 64.7\ {}^{+3.5}_{-3.7}\ SNU$$

$[pp|Ga] = 39.9 \pm 5.2$ SNU

(1 SNU = 1 interaction/s in a target that contains 10^{36} atoms of the neutrino absorbing isotope).

Реакторный зал ГГНТ

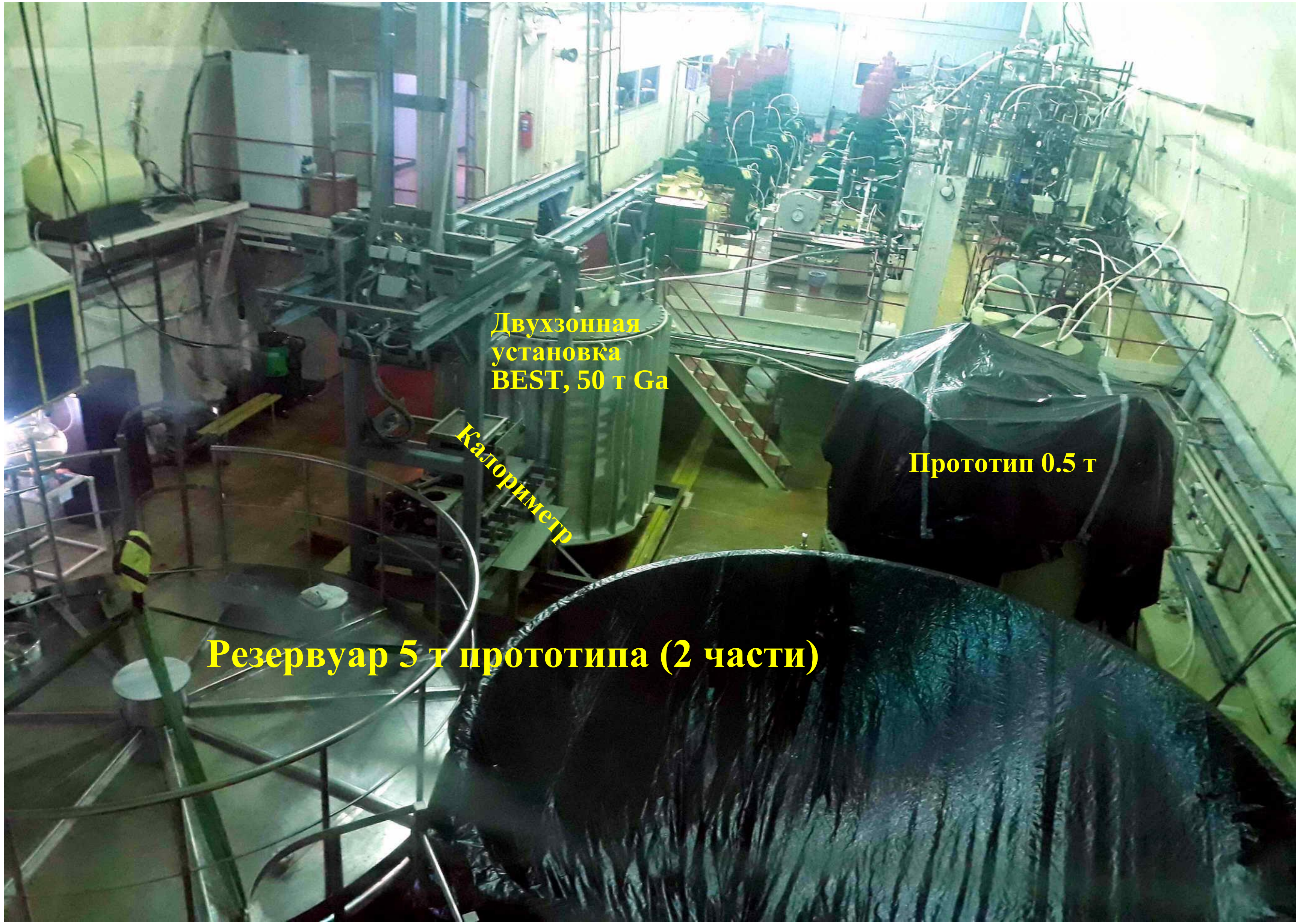

Gallium anomaly (GA)

GA – low neutrino capture rate in 4 calibration experiments of solar detectors of solar neutrinos SAGE and GALLEX with sources ^{51}Cr and ^{37}Ar

The BEST experiment confirmed the GA at a higher level of significance

	SAGE, m(Ga) = 13.1 m		GALLEX, m(Ga) = 30 m		BEST, m(Ga) = 48 m	
Source	^{51}Cr	^{37}Ar	^{51}Cr	^{51}Cr	^{51}Cr	
Activity, MCi	0.516	0.409	1.714	1.868	3.414	
$R = p_{measur}/p_{Expec}$	0.95 ± 0.12	0.79 ± 0.10	0.953 ± 0.11	0.812 ± 0.11	0.766 ± 0.05	0.791 ± 0.05

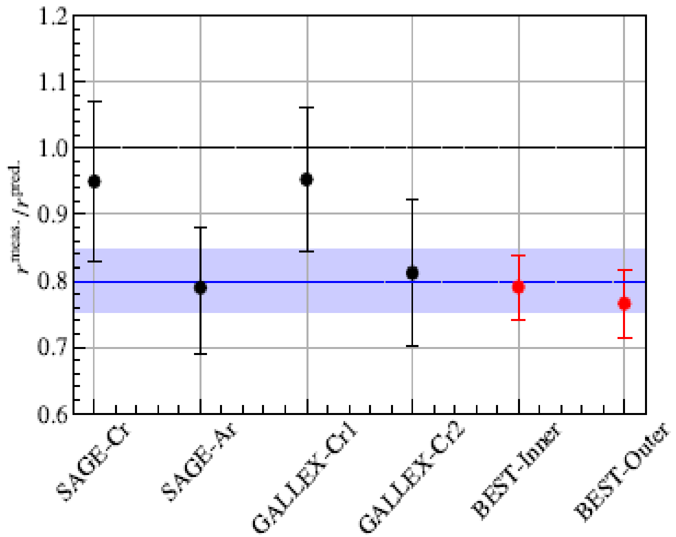

The total result $R_0 \pm \sigma_0 = 0.80 \pm 0.05$ (5.7%)
GA is confirmed at the level of > 4σ

vvgor_gfb1@mail.ru

Acceptable oscillation parameters based on the results of all Ga experiments with sources

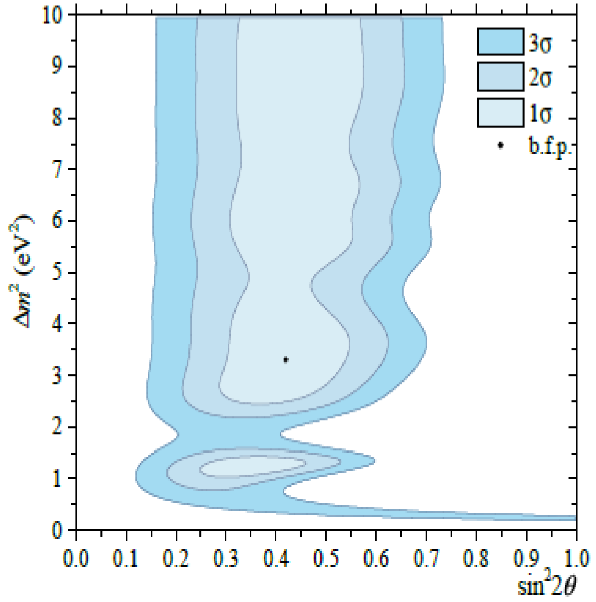

BF for 2 BEST measurements:
$\Delta m^2 = 3.3$ эВ^2 и $\sin^2(2\theta) = 0.42$

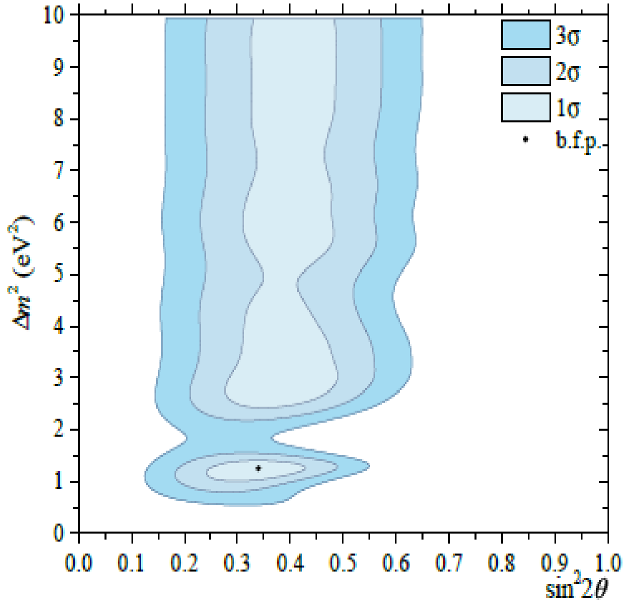

BF for (2 BEST + 2 SAGE + 2 GALLEX):
$\Delta m^2 = 1.25$ эВ^2 и $\sin^2(2\theta) = 0.34$

The total result $R_0 = 0.80 \pm 0.05$ (5.7%)
Ga anomaly confirmed at the level of $> 4\sigma$
The hypothesis of sterile neutrinos remains relevant
The parameter Δm^2 remains unknown (> 1 eV^2)

vvgor_gfb1@mail.ru

Explanation of Gallium anomaly (GA)

1) *Statistical fluctuation*
2) *Systematics of experiments*
3) *Overestimated neutrino capture cross section in Ga*
4) *New physics*

1) *After the BEST experiment, the probability of stat. fluctuations is suppressed at a level of* $> 4\sigma$
2) *Systematics verified by many independent experiments*
3) *The neutrino capture cross section has been measured at accelerators and has been calculated independently by several authors.*
4) *The main hypothesis from new physics is short-baseline oscillations into sterile states, which also explain anomalies obtained in other experiments – LSND, MiniBooNE, short-baseline reactor antineutrino measurements*

$$P_{ee} = 1 - \sin^2 2\theta \cdot \sin^2 (1.27 \frac{\Delta m^2 (eV^2) \cdot L(m)}{E_\nu (MeV)})$$

The oscillation parameters (Δm^2, $\sin^2 2\theta$) are currently the subject of searches in short-baseline neutrino experiments

The new BEST-2 experiment

A detailed study of GA
The main hypothesis is sterile oscillations
But also determine the dependence of GA on neutrino energy

Changes compared to BEST:

1) *A ^{58}Co source with a neutrino energy of 1500 keV, 2 times higher than that of ^{51}Cr (750 keV)*
2) *Three independent target zones - a more distance-sensitive target (there were 2 zones)*

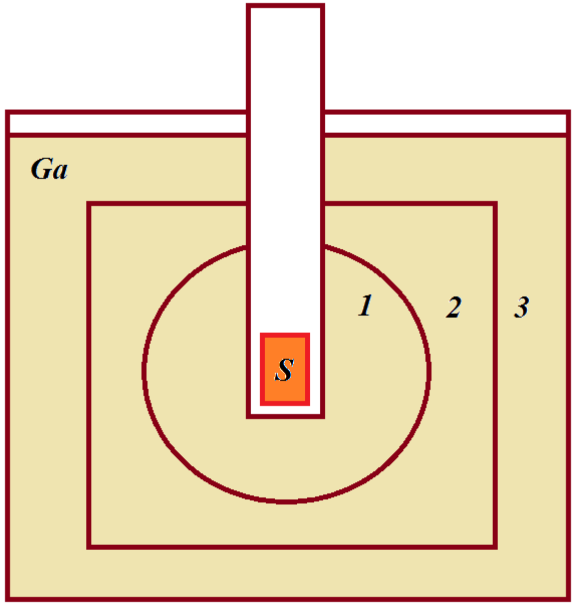

For the oscillation hypothesis:

- an increase in neutrino energy increases the width of the sensitivity region in terms of the parameter Δm^2

- increasing the number of target zones gives an unambiguous determination of the parameter Δm^2 in the sensitivity region

vvgor_gfb1@mail.ru

Sensitivity regions for searching oscillation parameters in the BEST-2 experiment

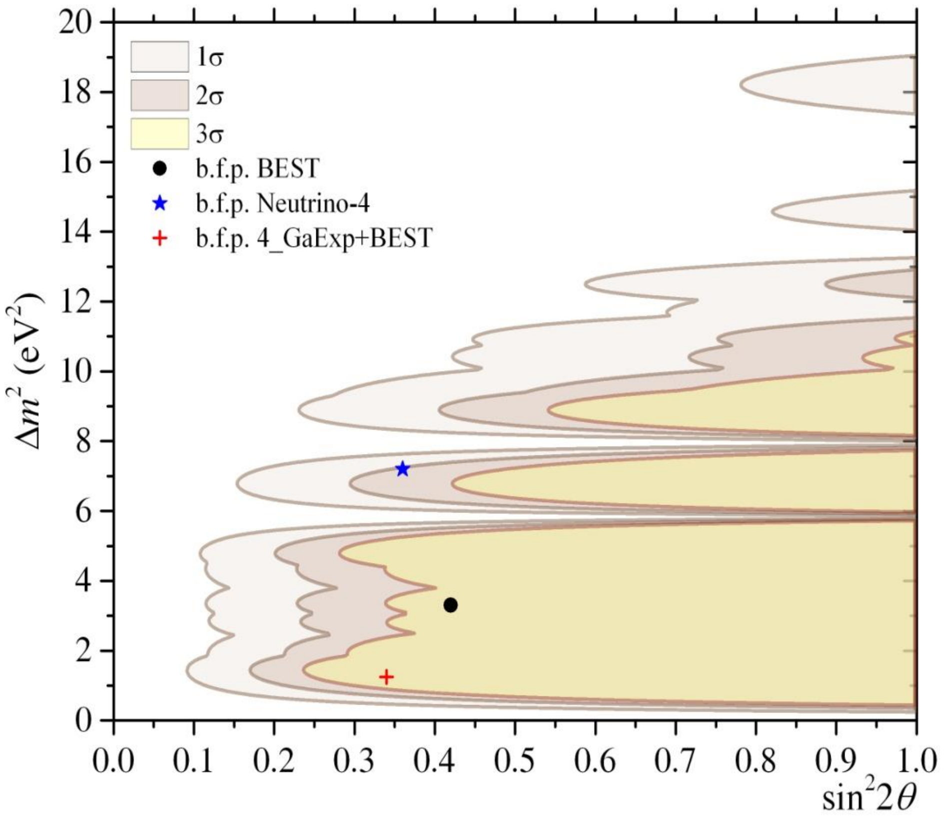

Within the sensitivity regions, the oscillation parameters can be defined:

within the boundaries of the 2σ region – with a significance level of 3σ, i.e. the parameters found in the analysis will coincide with the real ones at a significance level of 3σ

Thus, if the oscillation parameters coincide with any of the BF parameters of the Ga source experiments, as well as Neutrino-4, then they will be determined in the new experiment.

vvgor_gfb1@mail.ru

Why are 3 target zones needed?

The dependence of capture rates in three zones of the Ga target on the parameter Δm^2 for an amplitude of $\sin^2\theta = 0.30$ is shown.

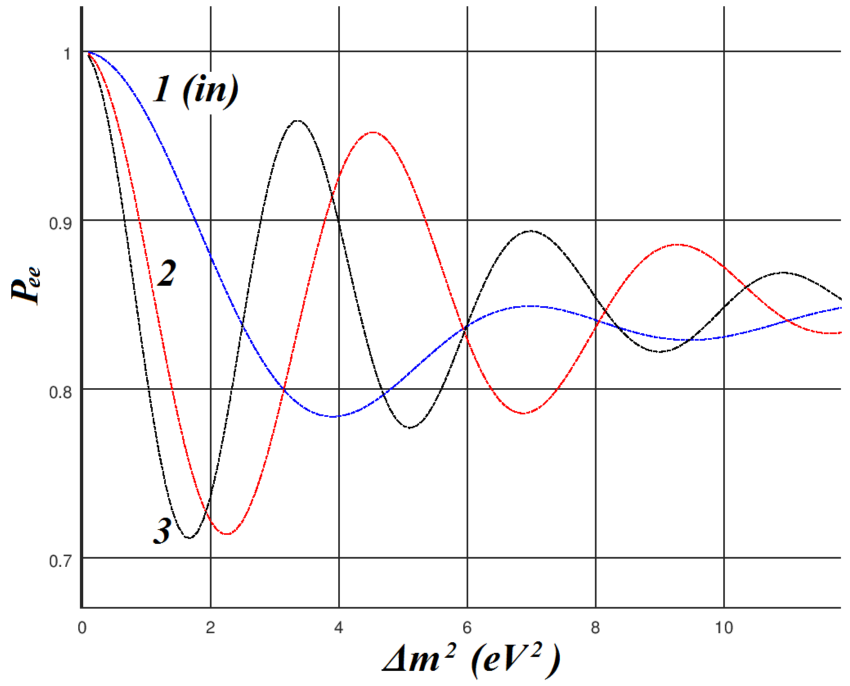

In the region of sensitivity to the determination of oscillation parameters, we obtain an unambiguous definition of the parameter Δm^2

The ratio of capture rates in different target zones:

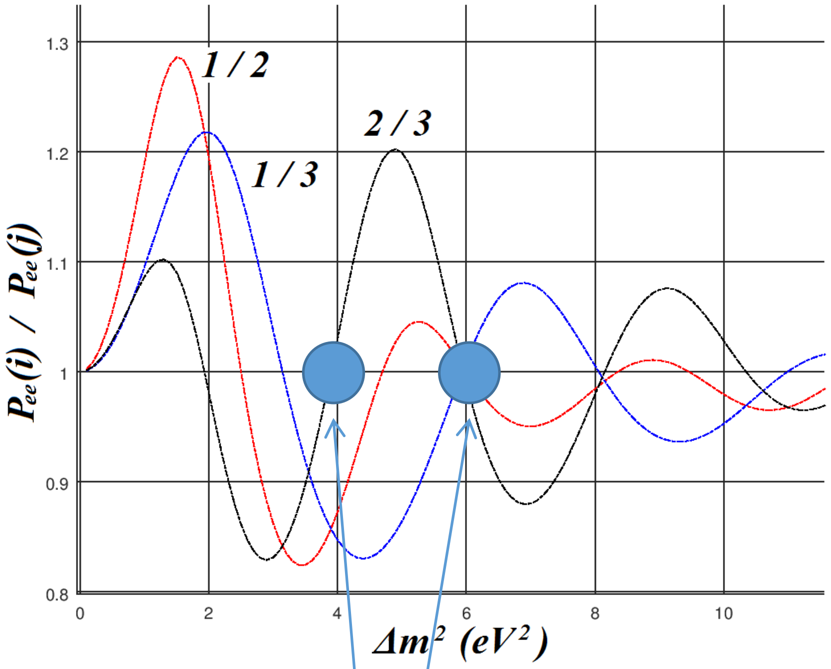

Sensitivity disappears in areas where the capture rates in all zones are equal

vvgor_gfb1@mail.ru

Source production

In a fast neutron reactor:

$$^{58}_{28}Ni(n,p)^{58}_{27}Co$$

Cross section of (p,n) reaction σ = 0.1439 barn

^{58}*Ni in natural Ni* 68.27 %

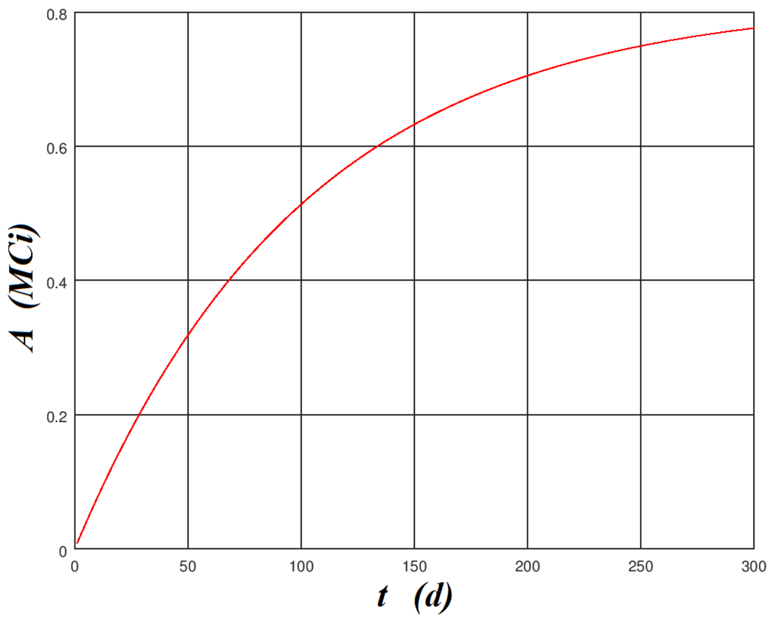

Production of ^{58}Co activity in a fast neutron flux $\Phi = 2{\cdot}10^{15}$ cm^{-2}s^{-1} from 15 kg of natural nickel

Fast neutron fluxes in reactors:

БОР60 (НИИАР) $3.7{\cdot}10^{15}$ cm^{-2}s^{-1}
БН600 $2.3{\cdot}10^{15}$ cm^{-2}s^{-1}

Activity A = 400 kCi
can be accumulated in ~70 days

At the same time, ^{60}Co is produced from
^{60}*Ni(σ = 0.040 barn)*
The activity of ^{60}Co will be ~ 250 times less

Density Ni - ρ = 8.90 g/cm3
Volume of 15 kg Ni - V = 1.7 l
Volume of ^{51}Cr source in BEST - V = 0.6 l

vvgor_gfb1@mail.ru

Photon activity and source heat

Gamma line of ^{58}Co:

E_γ, keV	511	810.76	864	1674.7
Branching ratio f, %	29.88	99.44	0.70	0.528

Heat dissipation: ~ 1 MeV / decay ^{58}Co = 593 W / 100 kCi = ***2.4 kW/ 400 kCi***
The heat dissipation in the BEST was ***740 W / 3.4 MCi***

For safe operation, the source will be surrounded by passive shield:
(3 cm W + 10 cm Pb) - 2.3 hours of operation at a distance of 1 m from the source

Radioactive impurities contribute to

- *heat generation (and error in measuring the source activity)*
- *background radiation, which must be protected from*

Enrichment of the source material significantly reduces the amount of impurities:
The impurities in the source in BEST contributed to the heat release in the order of $5 \cdot 10^{-6}$

vvgor_gfb1@mail.ru

Large-volume scintillation detector (~10 kt) at the BNO for recording natural fluxes of low-energy neutrinos (up to 100 MeV)

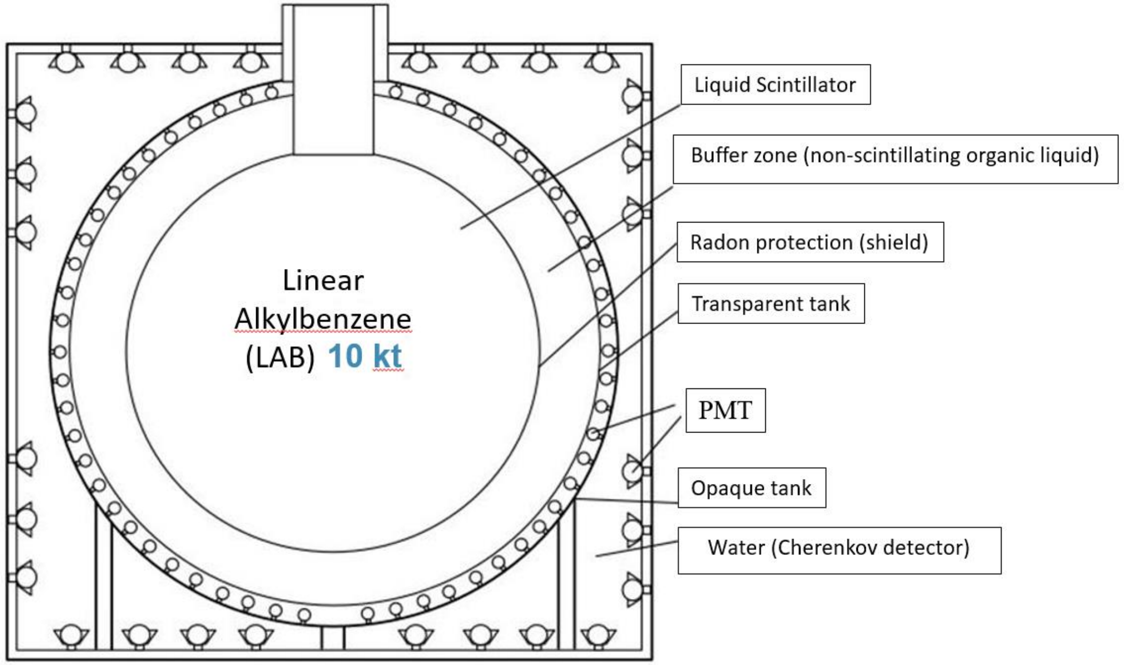

- Investigation of the spectrum of solar neutrinos and accurate measurement of neutrinos from CNO reactions;
- The study of the antineutrino flux emitted by uranium and thorium decay products (geoneutrinos) inside the Earth in order to determine the radiogenic component of the Earth's heat flux.
- Estimating the potassium content within the Earth using the electron spectrum from the recoil of neutrinos scattering on electrons, similar to solar neutrinos;
- Testing the hypothesis of a nuclear fission chain reaction taking place in the core of the Earth by looking for the "georeactor" antineutrino flux.
- Studying the dynamics of a supernova explosion by recording the intensity and spectrum of a neutrino burst (in the case of a burst);
- The search for the anisotropic flux of antineutrinos that has accumulated in the universe over millions of years due to gravitational collapses of the nuclei of massive stars and the formation of neutron stars and black holes.
- Measurement of the total flux of antineutrinos from all nuclear reactors on Earth and study of their oscillations.

Laboratory of Low Background Research

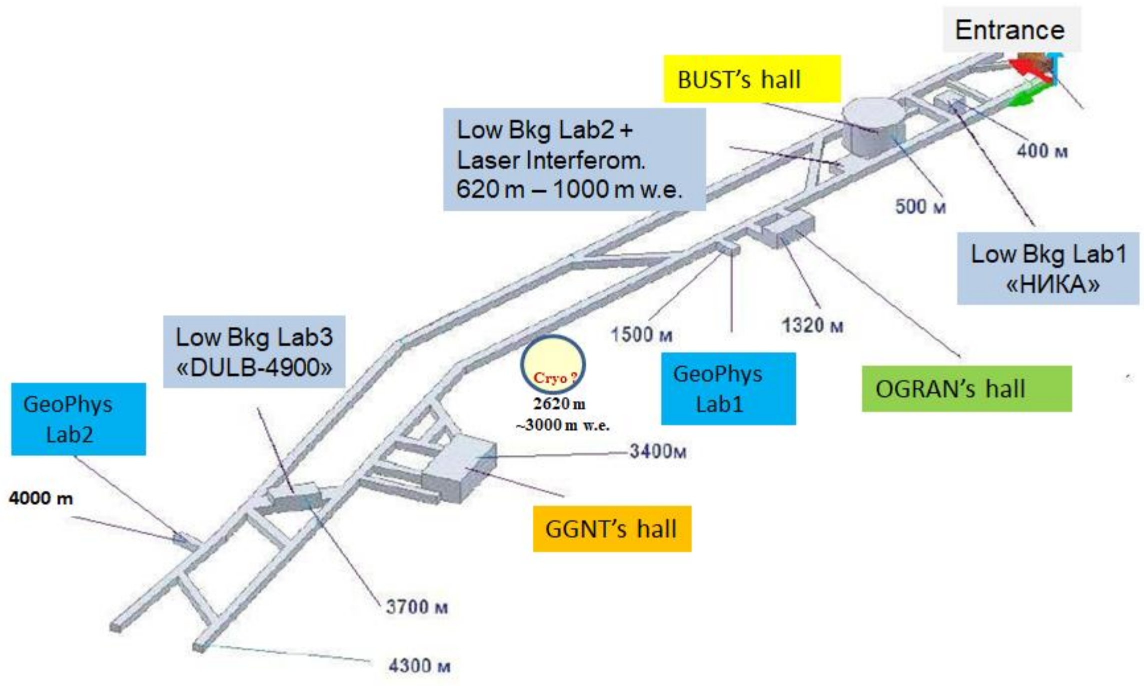

The main tasks of the laboratory :

- Experiments on the search for double beta decay (2K- capture ^{78}Kr, ^{124}Xe, AMoRE, GERDA)
- Measuring the radioactivity of materials
- Radon measurement (monitoring)
- Search for rare processes and decays

1) **НИ**зкофоновая **КА**мера (**НИКА**) – low-background chamber, at a distance of 385 meters from the entrance (660 m w. e.), cosmic rays are reduced by a factor of ~ 2×10^3 times
2) **КА**мера **ПР**ецизионных **ИЗ**мерений (**КАПРИЗ**) – low-background chamber, at a distance of 620 meters from the entrance (1000 m w. e.), cosmic rays are reduced by a factor of ~ 8×10^3 times
3) Deep Underground Low-background laboratory (**DULB-4900**) at a distance of 3670 meters from the entrance (4900 m w.e.), cosmic rays are reduced by a factor of ~ 1×10^7 times
4) Separate rooms: clean zone (class >600), instrumental rooms, rooms with HPGe and NaI detectors

Characteristics of deep underground low-background laboratory (DULB-4900)

Ju.M. Gavriljuk, A.M. Gangapshev, A.M. Gezhaev, V.V. Kazalov, V.V.Kuzminov, S.I. Panasenko, S.S. Ratkevich, S.P. Yakimenko
"Working characteristics of the New Low-Background Laboratory (DULB-4900, Baksan Neutrino Observatory)"
arXiv: 1204.6424 [physics.ins-det] 01 May 2012

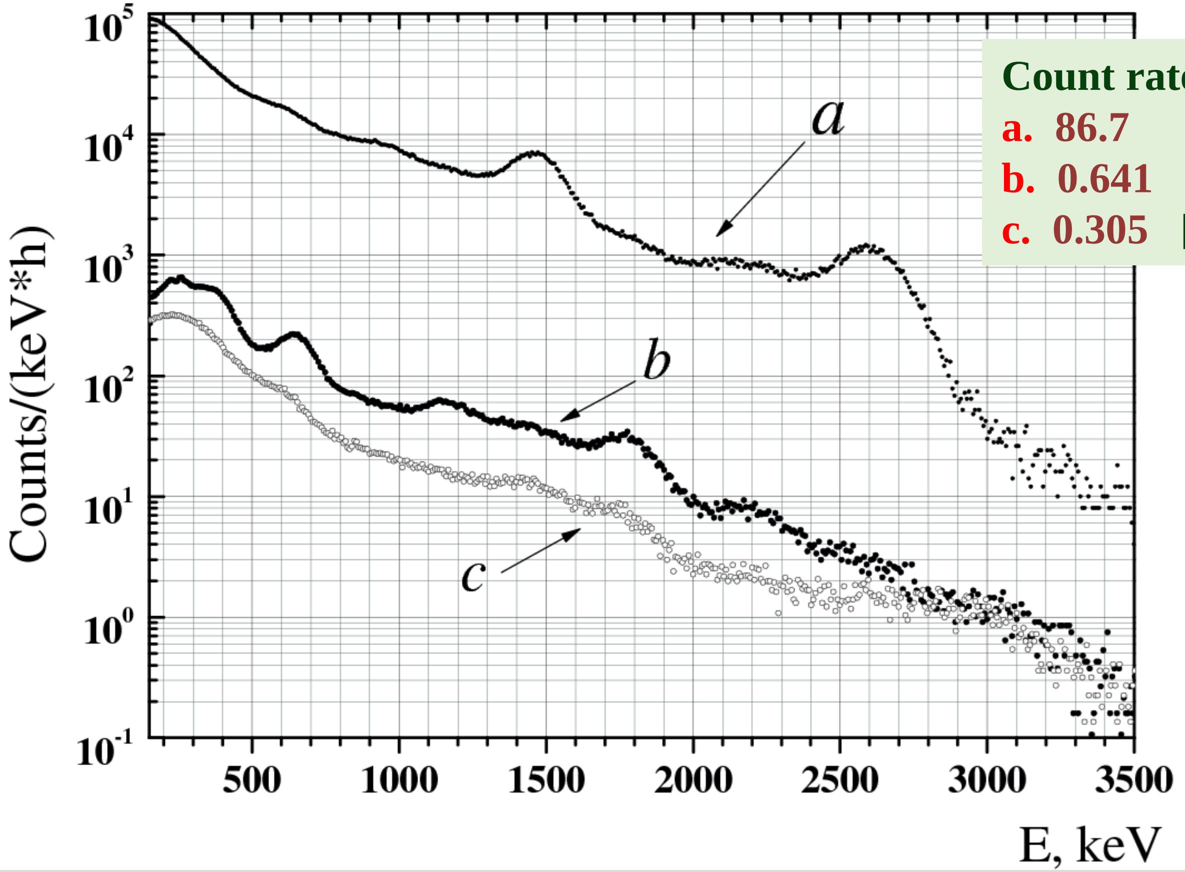

Count rate [0.3-3.0 MeV]
- **a. 86.7 [1/(s·kg)]**
- **b. 0.641 [1/(s·kg)]**
- **c. 0.305 [1/(s·kg)]**

Background spectra in the unshielded room of DULB (a), in a low-background box (b), in a low-background box with additional 15 cm Pb shield(c).
Crystal NaI(Tl) d=150 mm, h=150 mm, m=9.72 kg

Deep Underground Low-Background laboratory (DULB-4900)

The laboratory is located at a distance of 3700 m from the main entrance of the observatory tunnel in the hall with dimensions $\sim 6 \times 6 \times 40$ m^3. Thickness of the mountain rock over DULB corresponds to 4900 m w.e. and this deep location provides the cosmic ray flux reduction with the factor of about 10^7.

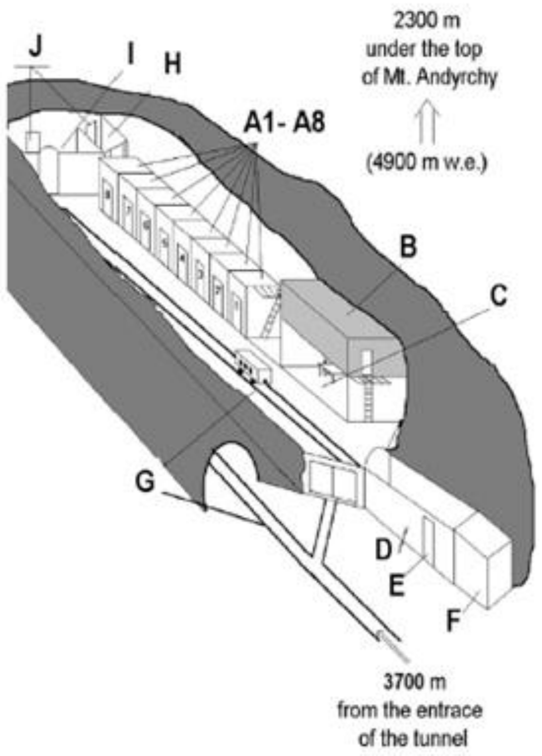

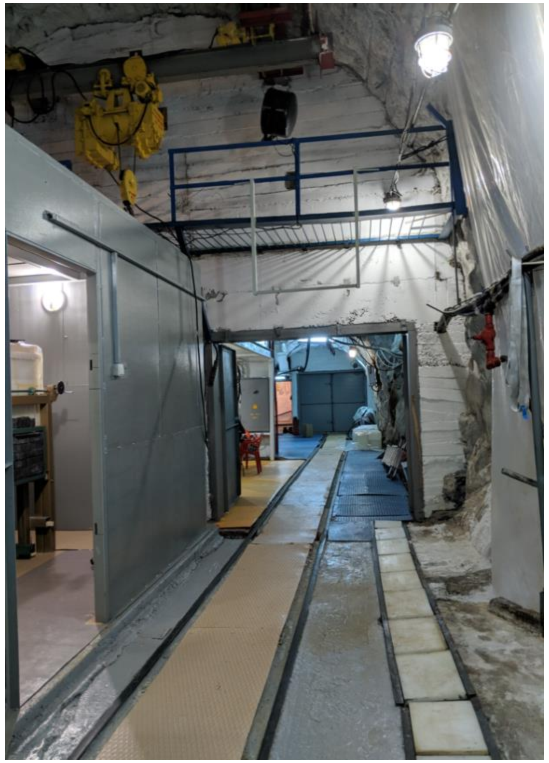

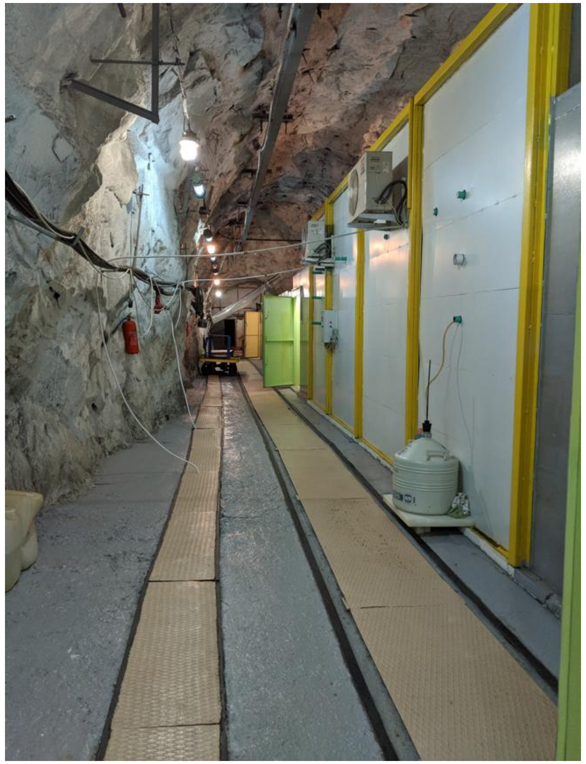

Schematic view of DULB-4900: A1-A8 - counting chambers; B - air condition equipment; C - engineering and processing facility; D - buffer area; E - entrance; F - bathroom; G - electric-driven wagon railway; H - fire-fighting equipment; I - electrical and process equipment; J - emergency exits.

Ju.M. Gavriljuk, A.M. Gangapshev, A.M. Gezhaev, V.V. Kazalov, V.V. Kuzminov, S.I. Panasenko, S.S. Ratkevich, A.A. Smolnikov, S.P. Yakimenko "Working characteristics of the New Low-Background Laboratory (DULB-4900)". Nuclear Instruments and Methods in Physics Research A 729 (2013) pp.576-580

Ultra-low background gamma-spetrometer «СНЕГ»

Characteristics of HPGe detector

Detector	Ge-Nat
Type of crystal	Coaxial
Type of semiconductor	P-type
Mass, g	1056
External diameter, mm	64
Height, mm	67
The thickness of the dead layer, mm	≈1
The effective mass, g	952
The wall thickness of the cryostat, mm	1
The ratio Peak / Compton (1332 keV)	54.8
The energy resolution, keV (1332 keV) at technical passport	2.32

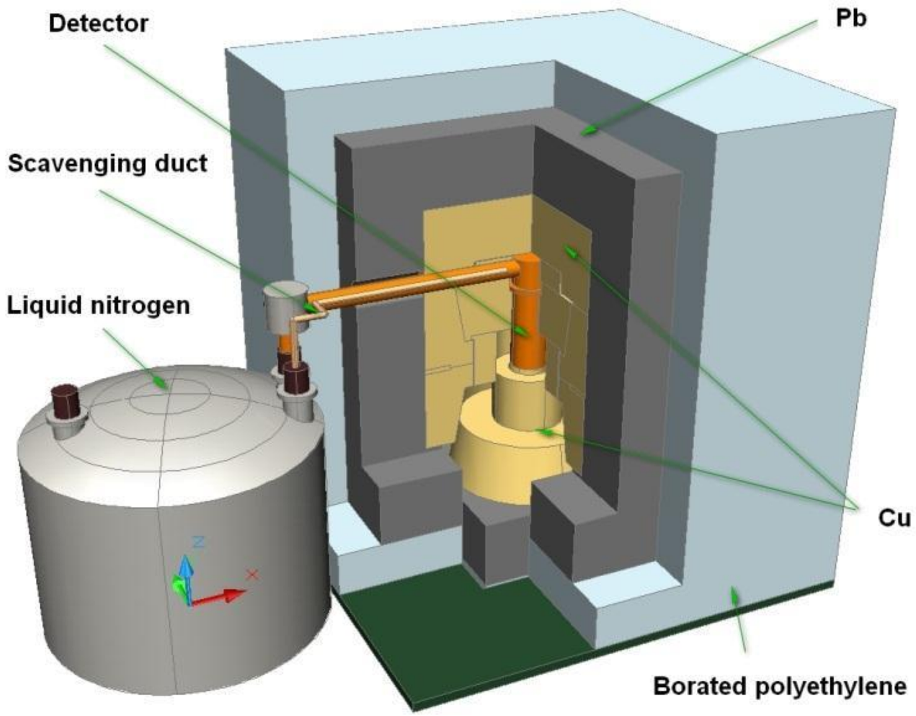

Low-background shield is consists of: 80 mm of polyethylene, 1 mm of cadmium (Cd), 150 mm of lead (Pb) and 180 mm of copper (Cu)

Candidates for measurement of $2\nu 2\beta^+$-decay

Transition	E_{2K}, MeV	Isotopic abundance, %
$^{78}Kr \to ^{78}Se$	2.867	0.35
$^{96}Ru \to ^{96}Mo$	2.724	5.52
$^{106}Cd \to ^{106}Pd$	2.771	1.25
$^{124}Xe \to ^{124}Te$	2.866	0.10
$^{130}Ba \to ^{130}Xe$	2.610	0.11
$^{136}Ce \to ^{136}Ba$	2.401	0.20

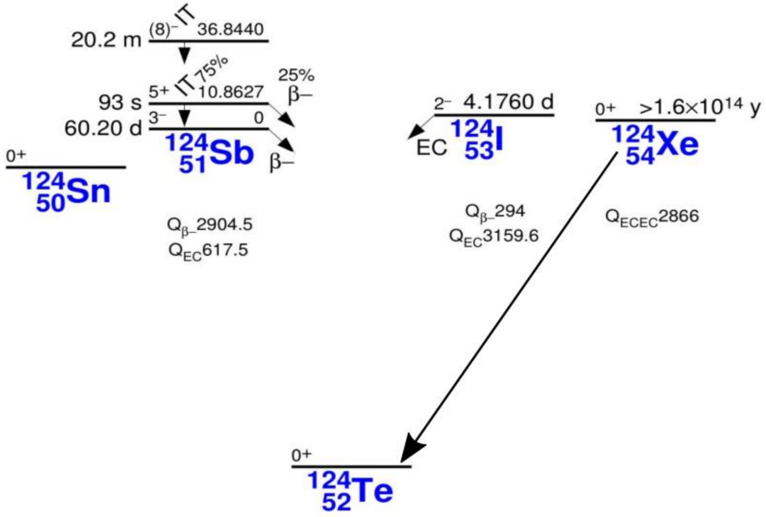

$(Z, A) \to (Z-2, A) + 2\beta^+ (+ 2\nu_e)$,

$e_b + (Z, A) \to (Z-2, A) + \beta^+ (+ 2\nu_e)$,

$e_b + e_b + (Z, A) \to (Z-2, A) + 2\nu_e + 2X$,

$e_b + e_b + (Z, A) \to (Z-2, A)^* \to (Z-2, A) + \gamma + 2X$.

2K-capture Xe-124

$$^{124}_{54}Xe \xrightarrow{2e_k} {}^{124}_{52}Te^{**} + 2\nu\,(2,865(7)\,MeV)$$

Te*	Te*	
e_a	e_a	$0.142^2 = 0.020$
e_a	K	0.246
K	e_a	
K	K	$0.857^2 = 0.734$

$K_{ab} = 31.8$ keV
$E_{2k} = 64.46$ keV
$\omega_k = 0.857$ - characteristic quantum
$\omega_e = 0.142$ - Auger electron

Search area of 2K(2ν)-capture of Xe-124
from 64.46-13= 51.46(52) to 64.46+13=77.46

Te----------------> Te*+ Te***

K_{ab}=31.81 keV,		
$K_{\alpha1}$=27.47 keV	52.2%
$K_{\alpha2}$=27.20 keV	27.7%
$K_{\beta1}$=30.99 keV	16.2%
$K_{\beta2}$=31.70 keV	3.9%

The energies of characteristic photons and an Auger-electron in 2K-capture are determined under the assumption that the filling of the double vacancy of K-shell in one atom is identical to filling two K-shell vacancies, each in a separate atom; the total energy release being 64.46 keV.
The probability of the emission of two characteristic X-ray photons and auger electron equal to 73.4%.

PSD

86.5% of KX rays (28.802 keV) are absorbed at the distance of 50 mm from their origin. Extrapolated range for Auger electrons (5 keV) is 0.5 mm. Therefore electrons are absorbed almost immediately while X-rays pass far away, creating three separate clusters of ionization. Information on the primary charge distribution along counter radius is fully represented in the pulse shape.

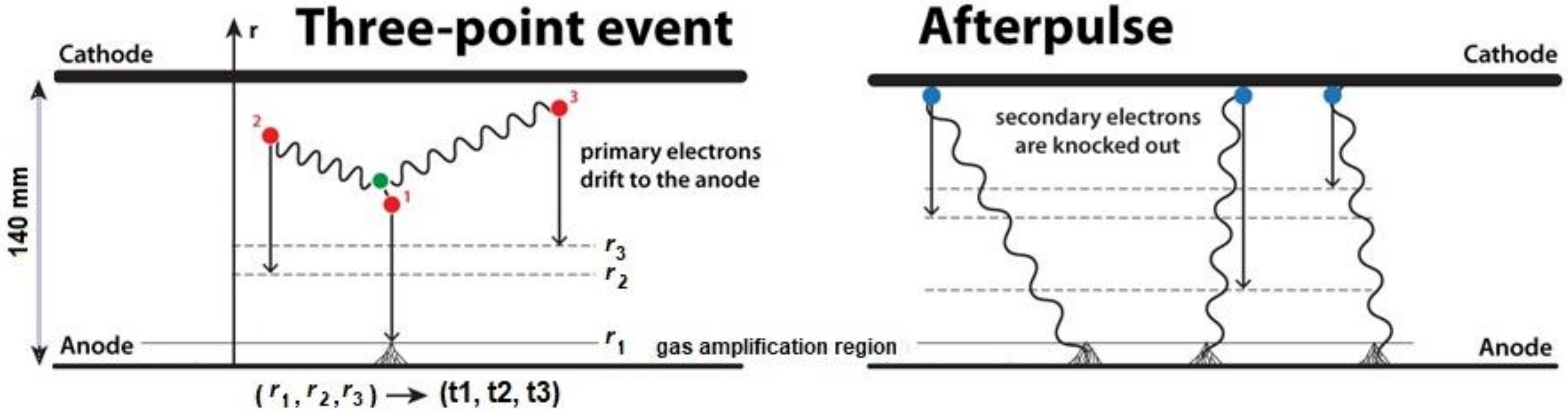

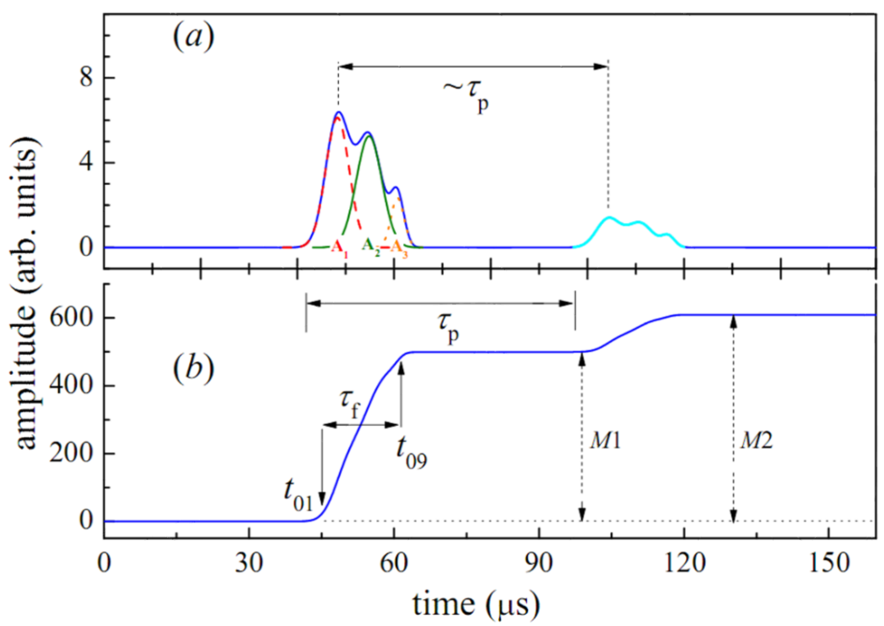

Three-point events have unique features and were the subject of study in the experiment.

$$\begin{Bmatrix} A_1 \\ A_2 \\ A_3 \end{Bmatrix} \Rightarrow \begin{Bmatrix} q_0 \\ q_1 \\ q_2 \end{Bmatrix}$$

$$\lambda = 100 \times M1/(M2 - M1)$$

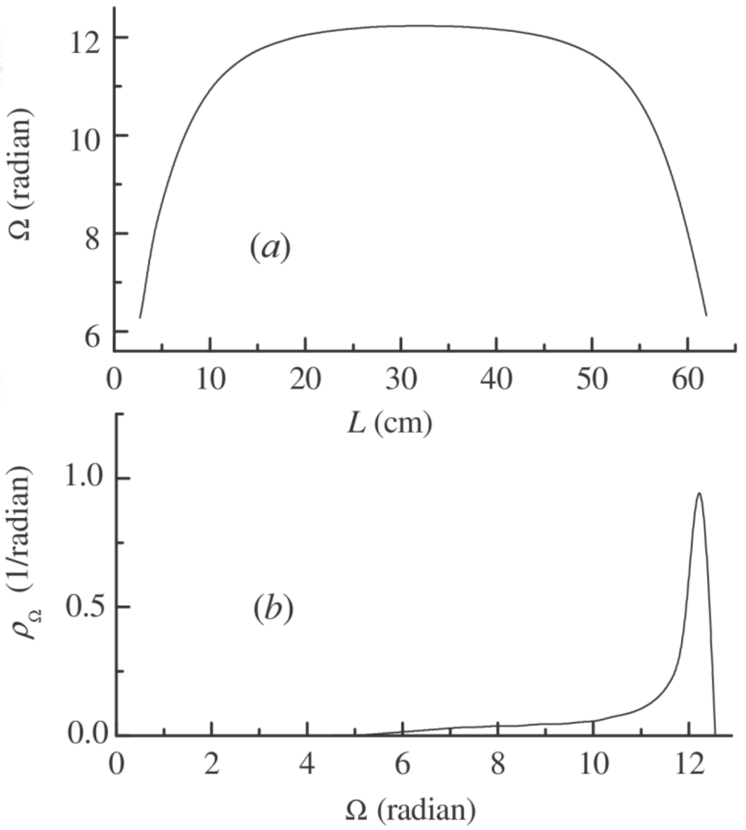

(a) The solid angle under which the interior surface of the counter from different points of an anode wire is visible. (b) The density of distribution of the solid angle for the points uniformly distributed along the anode wire.

Large low-background 10-liter copper proportional counter (CPC)

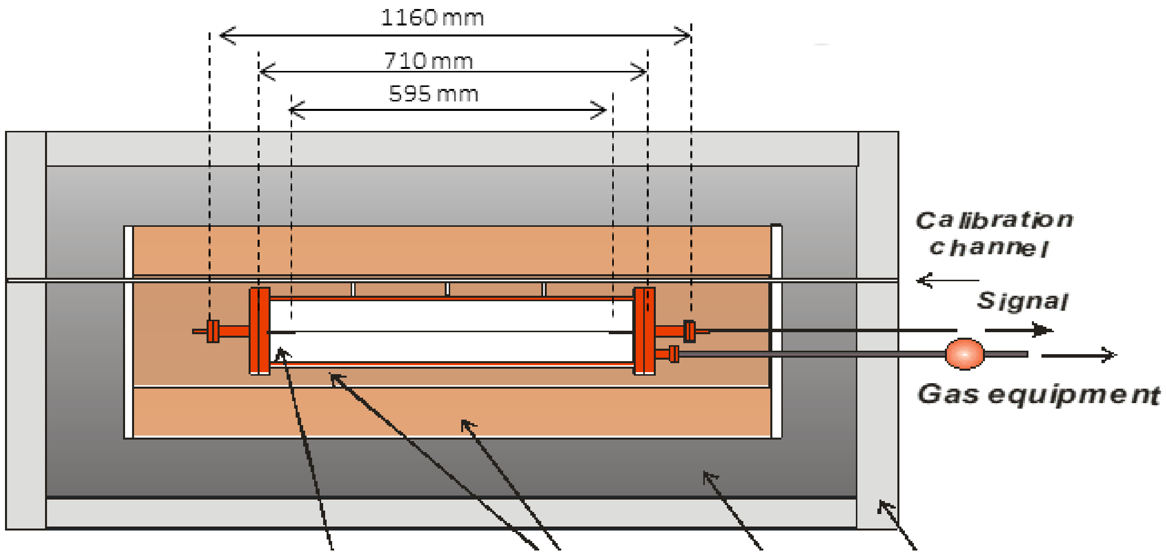

LowBG materials:

Xe	Cu	Pb	$(CH_2)n$
Source = Detector ~58 g	18 cm	15 cm	8 cm

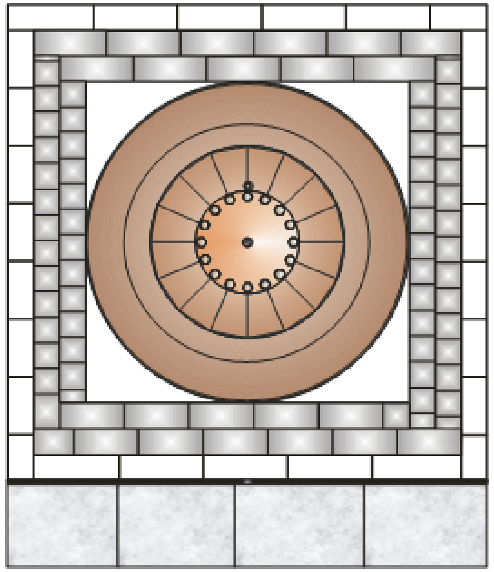

Main properties:

Casing material	Cu
Inner diameter, mm	137
Outer diameter, mm	150
Anode diam., mm	0.010
Total volume, L	10.3
Operating volume, L	8.77
Pressure, kPa	490.3
Capacity, pF	30.6
Anode resistance , Ohm	613
High voltage, V	3000

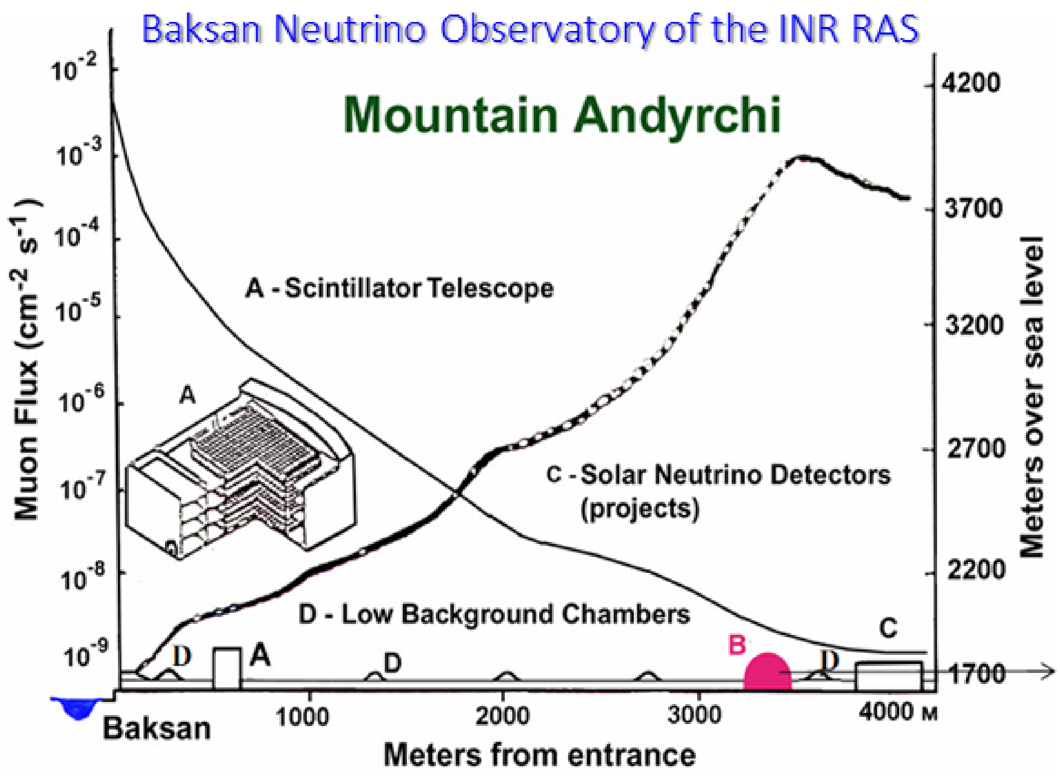

Proportional counter — Pre-amp (CSA) — Amp — Dig. Osc. LA-n20-12PCI — PC

Samples	Isotope content (vol %)				
	124	126	128	129	residual
Enrich. Xe (52.14 NL)	20.5	27.14	33.46	18.72	0.18

Comparison with previous experimental results and theoretical estimates

Experiment	2K-capture
XENON 1T (E. Aprile *et al.* Phys. Rev. C **106**, 024328)	**1.8×10^{22} лет**
XMASS-I (K. Abe, K. Hiraide, K. Ichimura, 2016г)	$\geq 4.7\times10^{21}$ лет
BNO INR RAS (2014г)	$\geq 4.67\times10^{20}$ лет
BNO INR RAS (2015г)	$\geq 2.5\times10^{21}$ лет
BNO INR RAS (2016г)	$\geq 4.6\times10^{21}$ лет
BNO INR RAS (2017г)	$\geq 7\times10^{21}$ лет

Theoretical predictions for 2e(2ν)-capture ^{124}Xe

2EC(2ν)×10^{21} yr.	Authors
2.9-7.3	M. Hirsch et al., *Z. Phys. A* 1999
7.0	O.A. Rumyantsev, M.H. Urin *Phys. Lett.B* 1998
7.1-18	S. Singh et al., *Euro. Phys. J. A* 2007
0.4-8.8	J. Suhonen *Journal of Physics G* 2013
61-155	A. Shukla, P.K. Raina *Journal of Physics G* 2007

Search for solar hadron axions

"Axions are among the most fascinating particles on the long list of those proposed but not yet observed or ruled out. Their existence would provide an elegant resolution of the strong CP problem. Even more exciting is the possibility that the missing mass needed to close the universe is composed of axions, and that axions are «cold dark matter» which seems to be necessary for galaxy formation. ..."
Mark Srednicki, "Axion couplings to matter (I). CP-conserving parts", Nucl. Phys. B260 (1985) 689-700.

"...the composite axion is a particular example of a "hadronic" axion, resulting from a theory where only exotic fermions carry $U(1)_{PQ}$ charges. Hadronic axions don't couple to leptons, which are neutral under $SU(3)xU(1)_{PQ}$. Nor do they couple to heavy quarks, which are integrated out of the theory above 1GeV, where QCD gets strong. Hadronic axions will still couple to nucleons as well as to photons. ..."
David B. Kaplan, "Opening the axion window", Nucl. Phys. B260 (1985) 215-226.

"The most attractive solution of the strong CP problem is to introduce the Peccei-Quinn global symmetry which is spontaneously broken at energy scale f_a. The original axion model assumed that f_a is equal to the electroweak scale. Although it has been experimentally excluded, variant "invisible" axion models are still viable in which f_a is assumed to be very large. ... Such models are referred to as hadronic and Dine-Fischler-Srednicki-Zhitnitskii axions. ...."
Shigetaka Moriyama, "Proposal to search for a monochromatic component of solar axions using ^{57}Fe", Phys. Rev. Lett. v.75 №8 (1995) 3222-3225.

Search for solar hadron axions

Solar Axions and How to Detect Them?

Stars could be intense **sources of axions**, thanks to a number of processes:

- Nuclear reactions of *pp*-chain (g_{AN})
- Thermal excitation of nuclei (g_{AN})
- Primakoff effect ($g_{A\gamma}$)
- Axion bremsstrahlung (g_{Ae})
- Compton-like process (g_{Ae})
- Atomic de-excitation/recombination (g_{Ae})

Due to the Sun's proximity to Earth the stellar **axion flux** at the Earth's surface will be **dominated by solar axions**.
Axions could be **detected** through reaction of **resonant absorption** by atomic nucleus (g_{AN}). The **relaxation** of excited nuclei would produce **γ-quanta and electrons**, detectable by conventional means.
Particular isotopes (^{57}Fe, ^{169}Tm, ^{83}Kr) possess **low-energy nuclear transitions** of M1-type, which allow for testing for axion masses in **1 — 10** keV range, consistent with the expected solar flux.
For our experiment ^{83}**Kr target** with **9.4** keV transition was used.

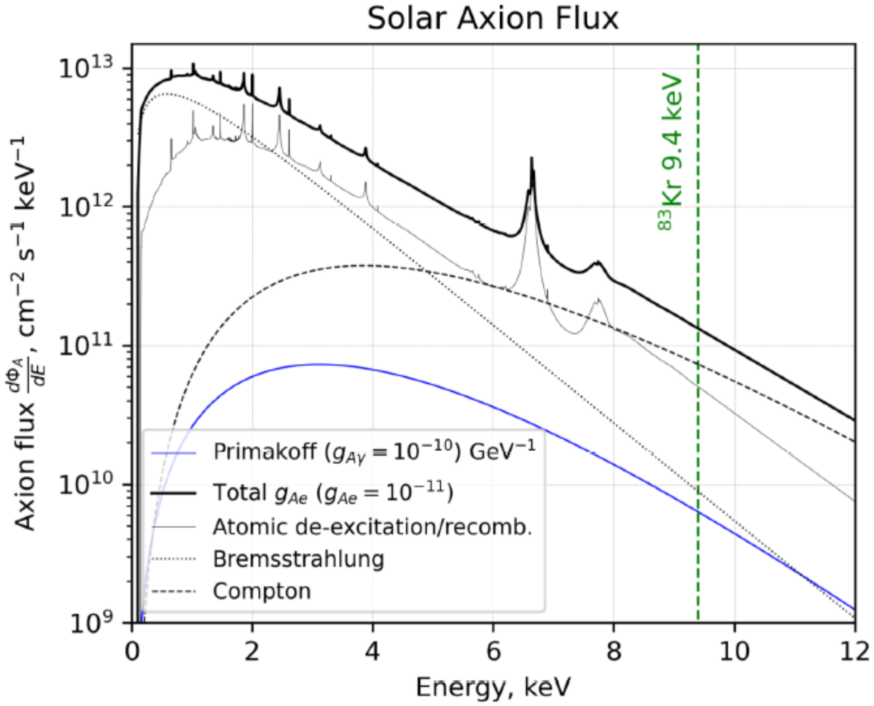

Search for solar hadron axions

Baksan Underground Facility and Experimental Setup

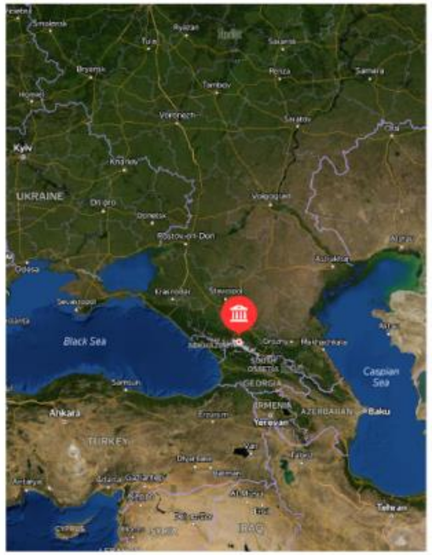

The experimental setup was located in the **low-background** laboratory of **Baksan underground facility** (4900 m. w. e). The large gas **proportional counter** consisted of **copper cylinder** ($l = 735$ mm, $\varnothing = 137 - 150$ mm) and was filled with **57** g of ^{83}Kr (**99.9**% enrichment).
The energy spectrum was acquired over **777** days of live-time. Since there was **no visible peak** in the region of interest, the **upper limit** on the amount of axion events was found to be $S_{lim} \leq 140$ at **90**% c. l.

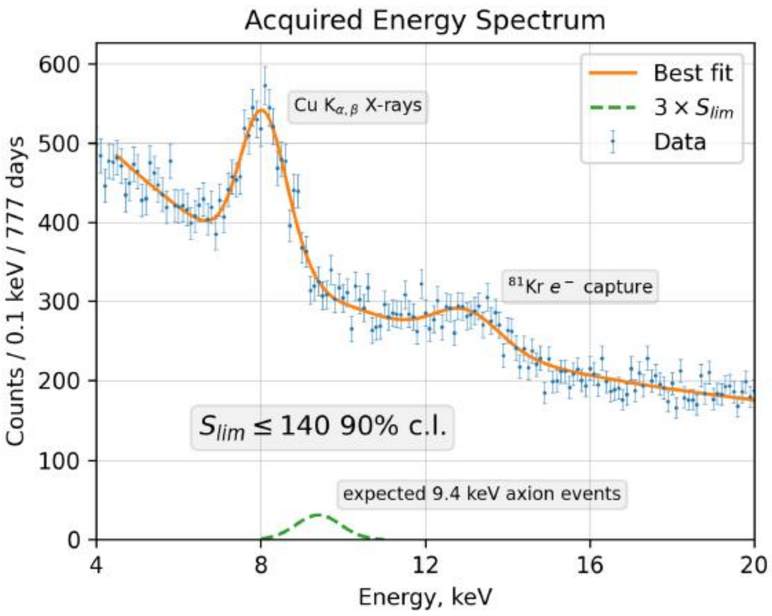

Search for solar hadron axions

Achieved Limits on Axion Couplings

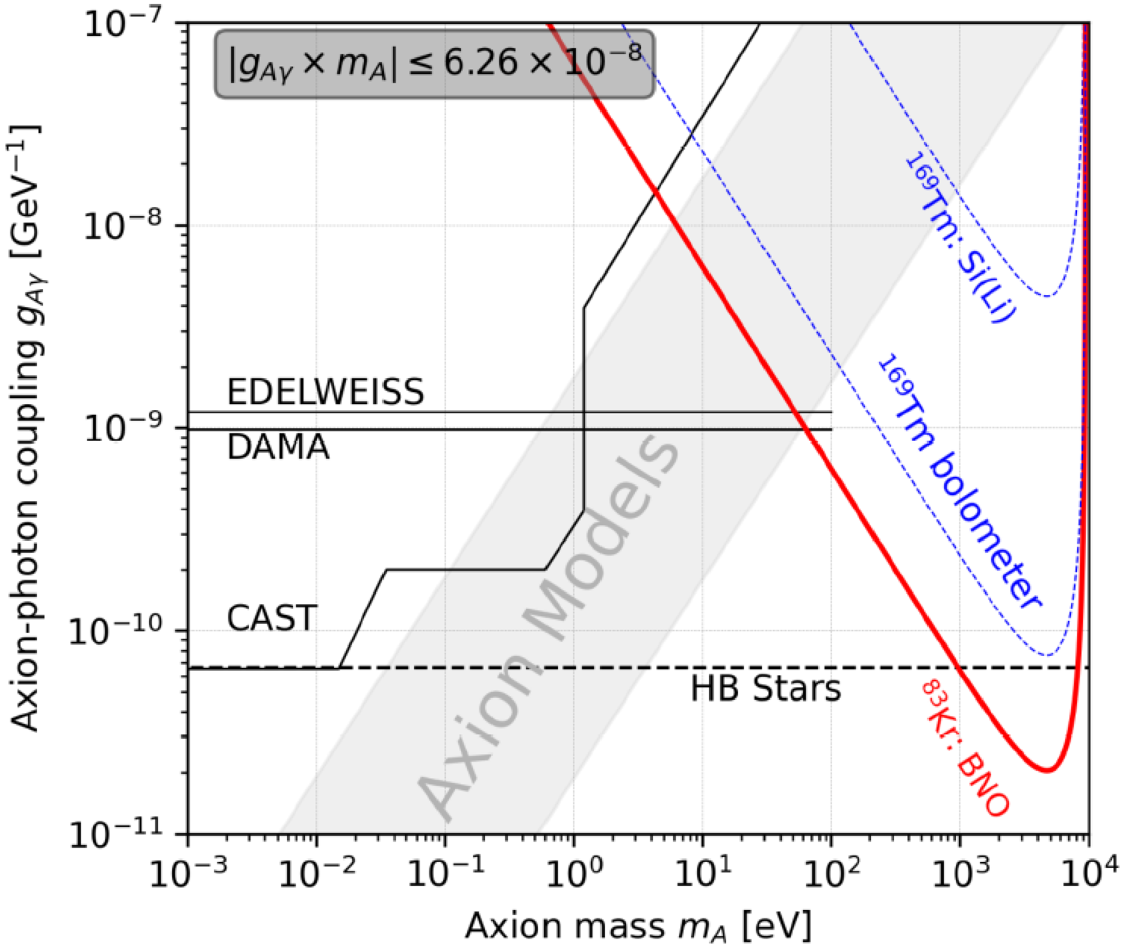

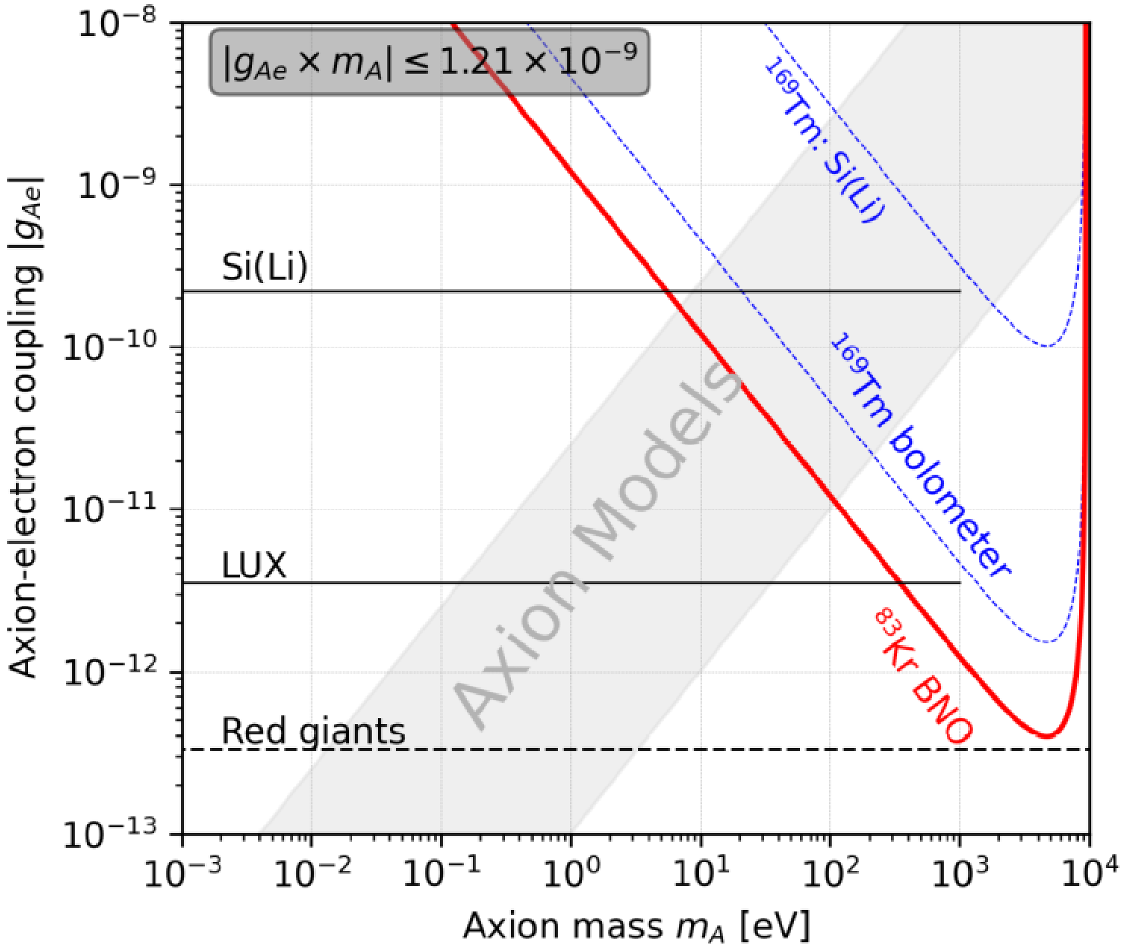

Flux of solar axions due-to Primakoff effect

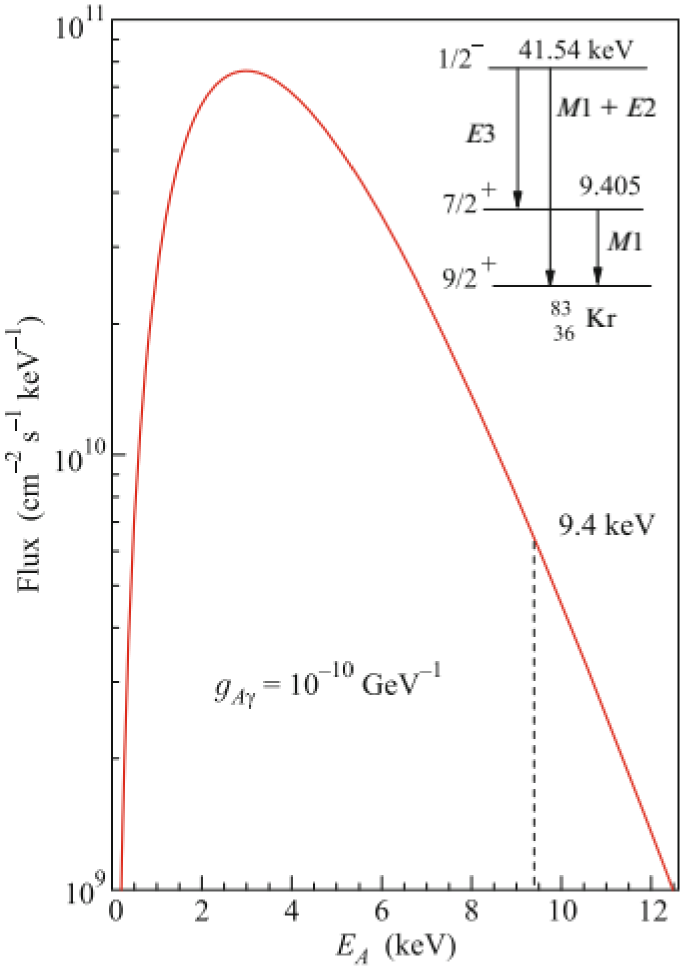

Fig. 1. (Color online) Energy spectrum of axions formed through the thermal-photon conversion in the solar-plasma field, derived for $g_{A\gamma} = 10^{-10}$ GeV^{-1}. The inset shows the scheme of ^{83}Kr levels.

$$\frac{d\Phi_A}{dE_A} = 6.02\times10^{30} g_{A\gamma}^2 E_A^{2.481} e^{-E_A/1.205}$$

1) V. Anastassopoulos et al. (CAST Collab.), Nat. Phys. 13, 584 (2017); arXiv:1705.02290v2
2) K. van Bibber, P. M. McIntyre, D. E. Morris, and G. G. Raffelt, Phys. Rev. D 39, 2089 (1989)

Rate of axion absorption by the ^{83}Kr nuclei:

$$R_A = 4.53\times10^{27} g_{A\gamma}^2 (\omega_A/\omega_\gamma)$$

$$6.70\times10^{27} g_{A\gamma}^2 (g_{AN}^3 - g_{AN}^0)^2 (p_A/p_\gamma)^3$$

In case of hadronic axion it gives:

$$R_A = 1.56\times10^{-7} m_A^4 (p_A/p_\gamma)^3$$

Result of measurements

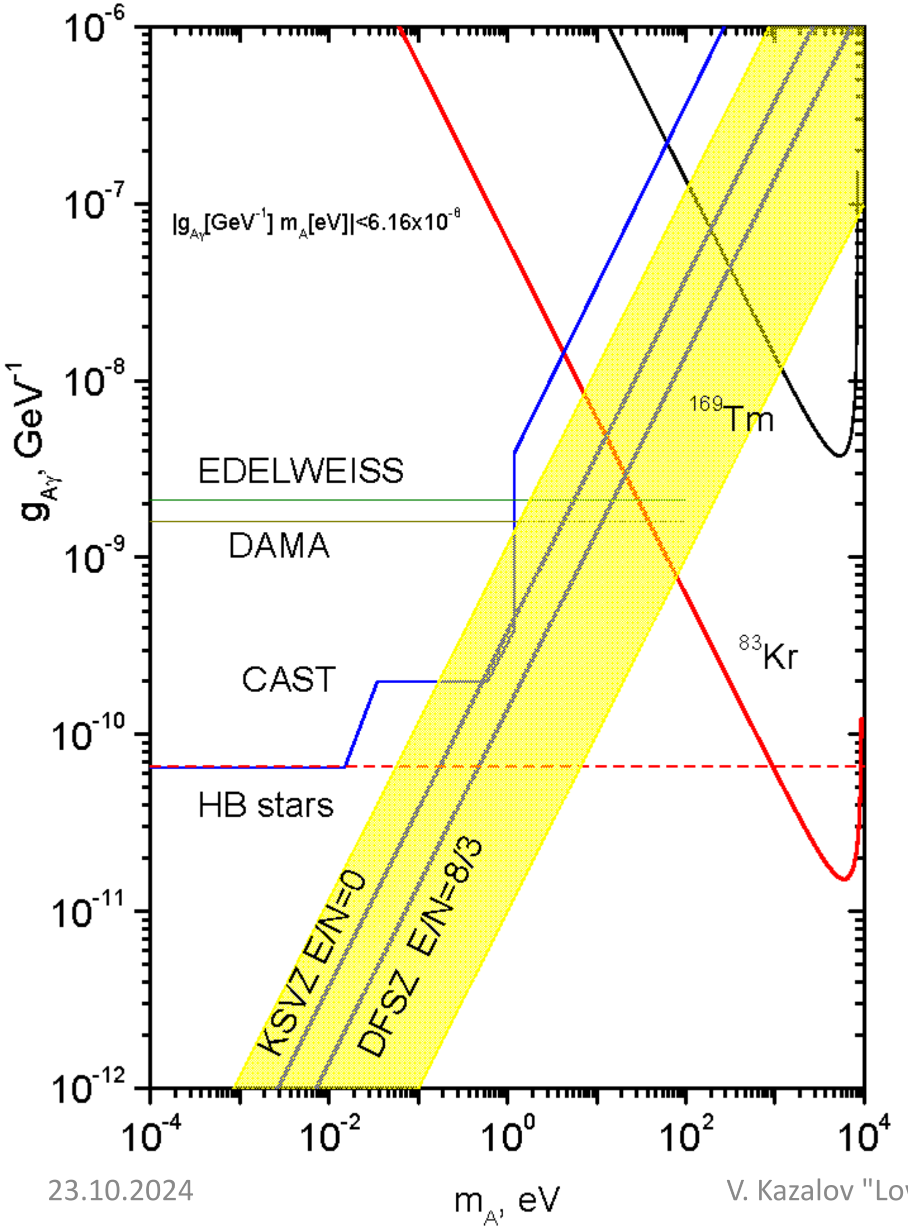

axions from ^{83}Kr:

$$\frac{\omega_A}{\omega_\gamma} \leqslant 9.9\times10^{-13}$$

$$|g^3_{AN}-g^0_{AN}|\leqslant 8.3\times10^{-7}$$

$$m_A \leqslant 64\,eV$$

axions due-to Primakoff effect:

$$|g_{A\gamma}(g^3_{AN}-g^0_{AN})|\leq 7.89\times10^{-16},$$

$$|g_{A\gamma}\times m_A|\leq 6.16\times10^{-8},$$

$$m_A\leq 12.6\,eV$$

AMoRE collaboration

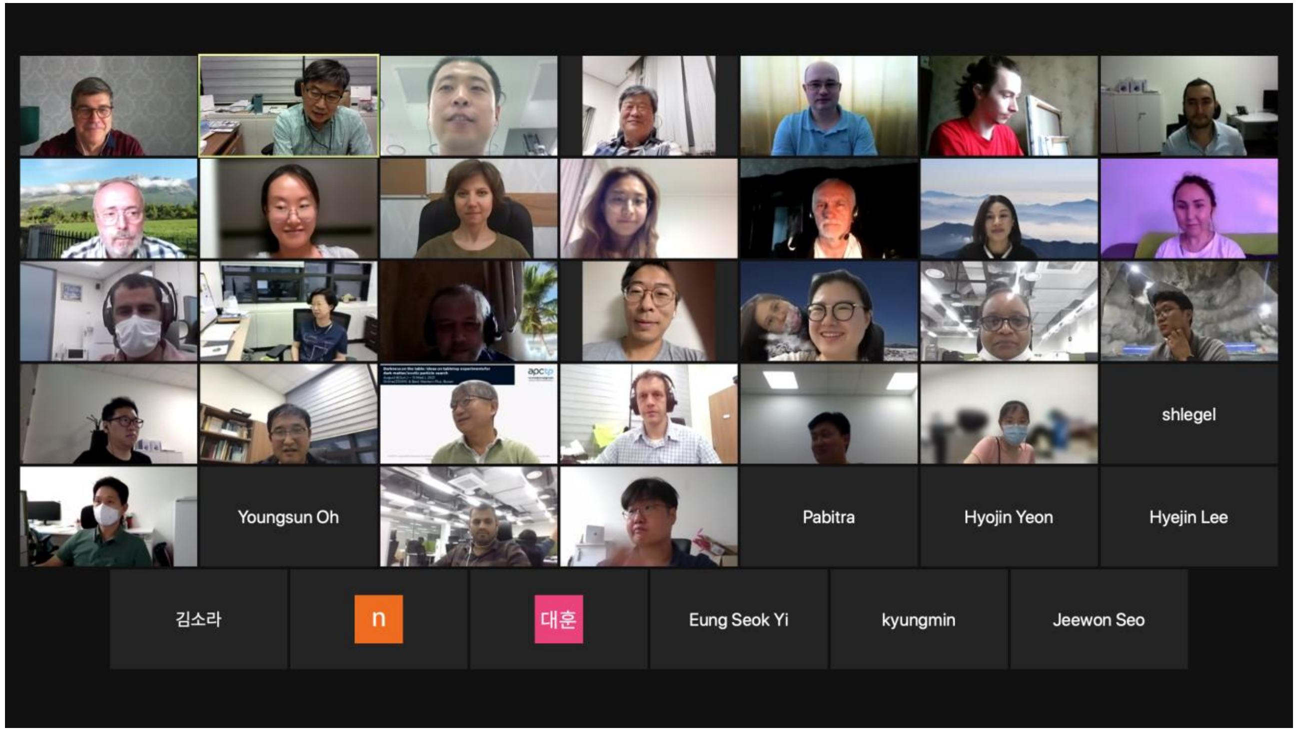

10 Countries, 26 Institutions - Korea, Germany, Ukraine, USA, Russia, China, Thailand, Indonesia, India, Pakistan

The AMORE-experiment's challenge

The goal of the **AMoRE** (**A**dvanced **Mo**-base **R**are process **E**xperiment) is to search for neutrinoless double beta decay (0υββ) of ^{100}Mo using Mo-based scintillating crystals and low-temperature sensors.

Experimental signature of 2νββ and 0νββ:

$$^{100}Mo \xrightarrow{2\nu\beta\beta} {}^{100}Ru + 2\beta^- + \bar{\nu}_e$$

$$^{100}Mo \xrightarrow{0\nu\beta\beta} {}^{100}Ru + 2\beta^-$$

$2\nu\beta\beta$ decay
- 2nd order beta decay
- Rare nuclear decay
- (>10^{18} years of half life)

$0\nu\beta\beta$ decay
- Massive neutrino
- Majorana particle
- Beyond the SM model
- >10^{25} years of half-life

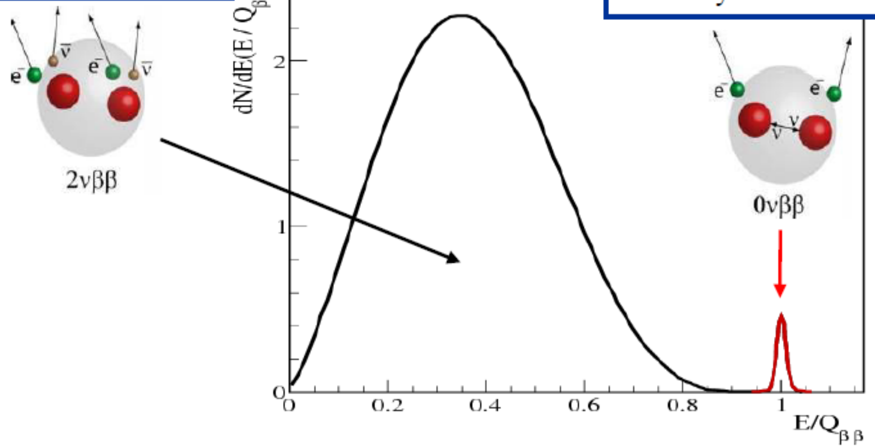

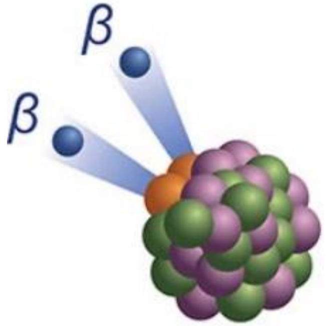

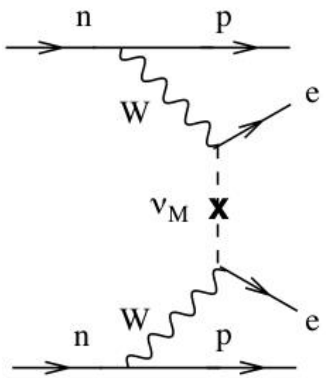

To observe 2νββdecay, the single β-decay must be energetically forbidden due to energy conservation constraint.

In total 35 isotopes available and > 9 of them can be used for 0νββ search.

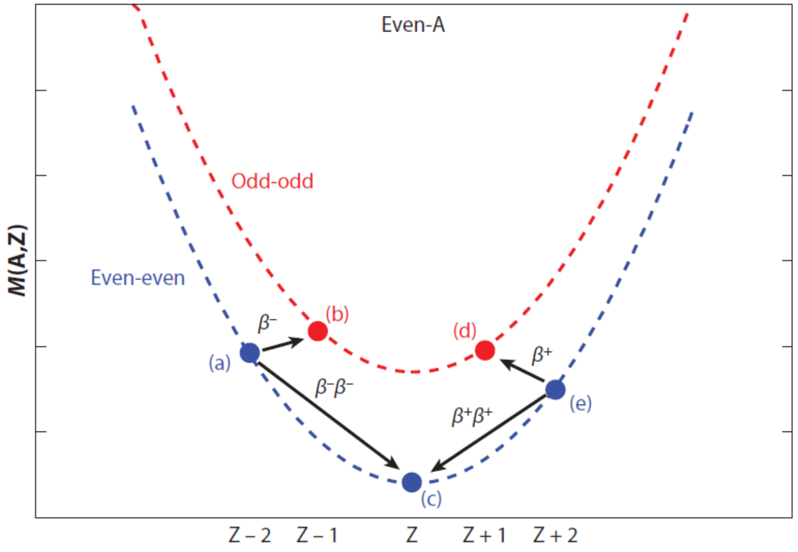

- Lepton-number violation (**ΔL=2**)
- The nature of neutrino mass (**Dirac or Majorana?**)
- Type of neutrino mass hierarchy (normal, inverted)
- CP-violation in the lepton sector

Principle of AMoRE detector

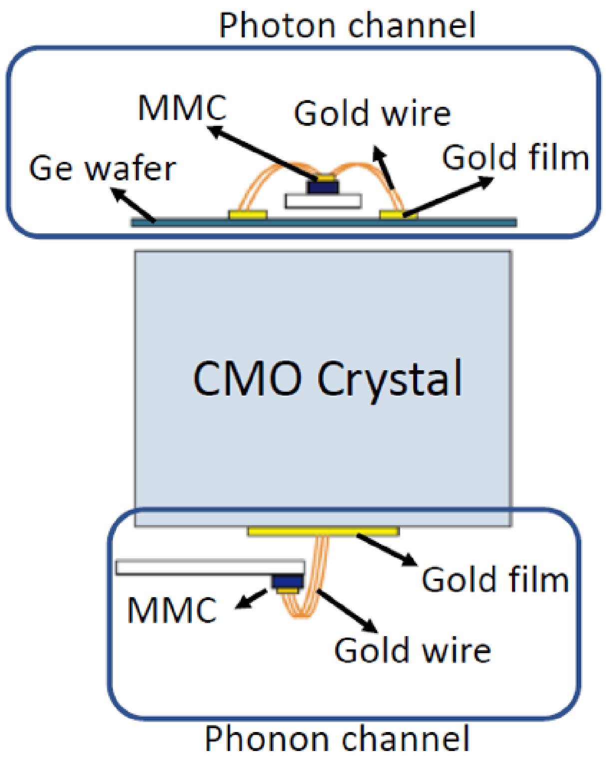

Scintillating crystal
- $^{48depl}Ca^{100}MoO_4$
- ^{100}Mo enriched: > 95 %
- ^{48}Ca depleted: < 0.001 %

MMC & SQUID
- MMC: Metallic Magnetic Calorimeter
- Magnetization changes with temperature.
- Magnetization change (flux) can be measured as a voltage by SQUID

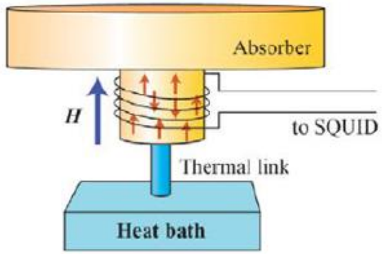

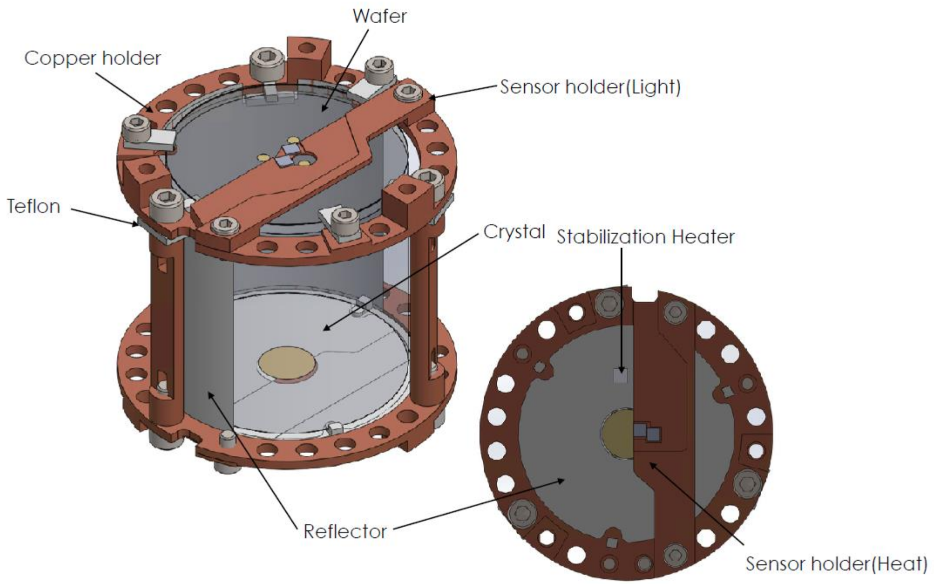

Detection process:
Energy → Temperature → Magnetization → Magnetic flux → **Voltage**

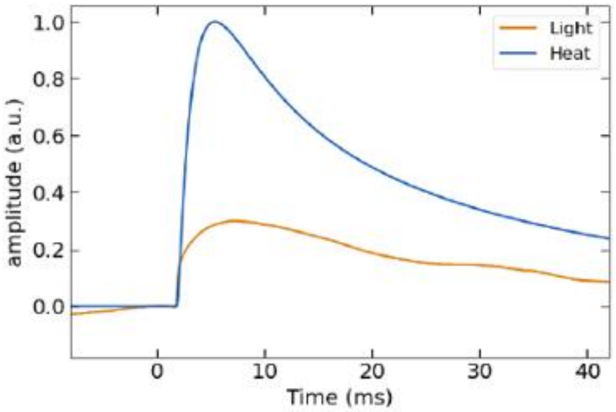

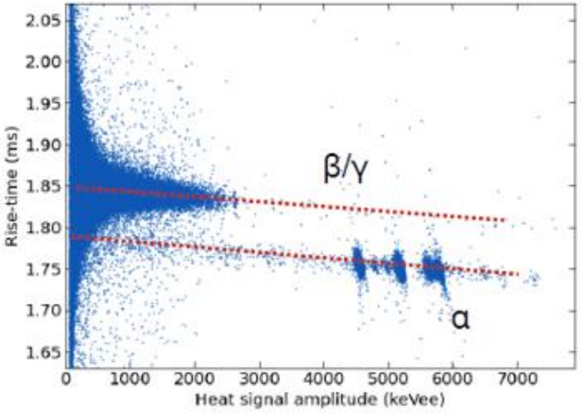

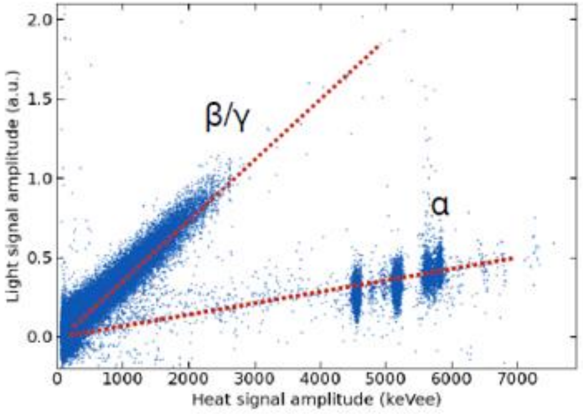

AMoRE project

Этапы эксперимента	Pilot	AMoRE-I	AMoRE-II
Crystal assembly		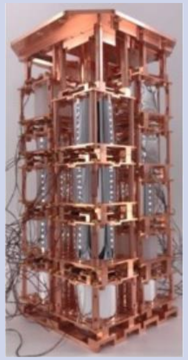	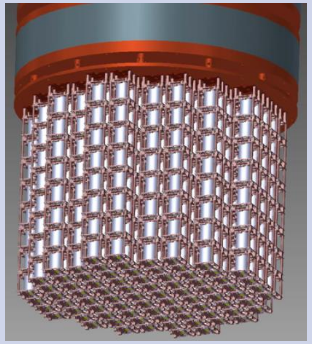
Crystals	$^{48depl}Ca^{100}MoO_4$ (CMO)	$^{48depl}Ca^{100}MoO_4$, $^{nat}Li_2{}^{100}MoO_4$ (LMO)	$^{nat}Li_2{}^{100}MoO_4$
Crystal/Mass	6/1,9 kg	18/6,2 kg	~ 400/150 kg
Background Goal (counts/keV/kg/yr.)	10^{-1}	$< 10^{-2}$	$< 10^{-4}$
Sensitivity , $T_{1/2}(\text{yr.})$	$1{,}0\text{x}10^{23}$	$7{,}0\text{x}10^{24}$	$8{,}0\text{x}10^{26}$
Sensitivity, neutrino mass $m_{\beta\beta}$(мэВ)	1200-2100	140-270	13-25
Scheduled Dates	2015-2018	2020-2022	2024-2027
Location	Yangyang Underground Laboratory (Y2L), S. Korea	Y2L	Yemi Underground Laboratory (YemiLab), S. Korea

Background spectra AMoRE-I after alpha background rejection

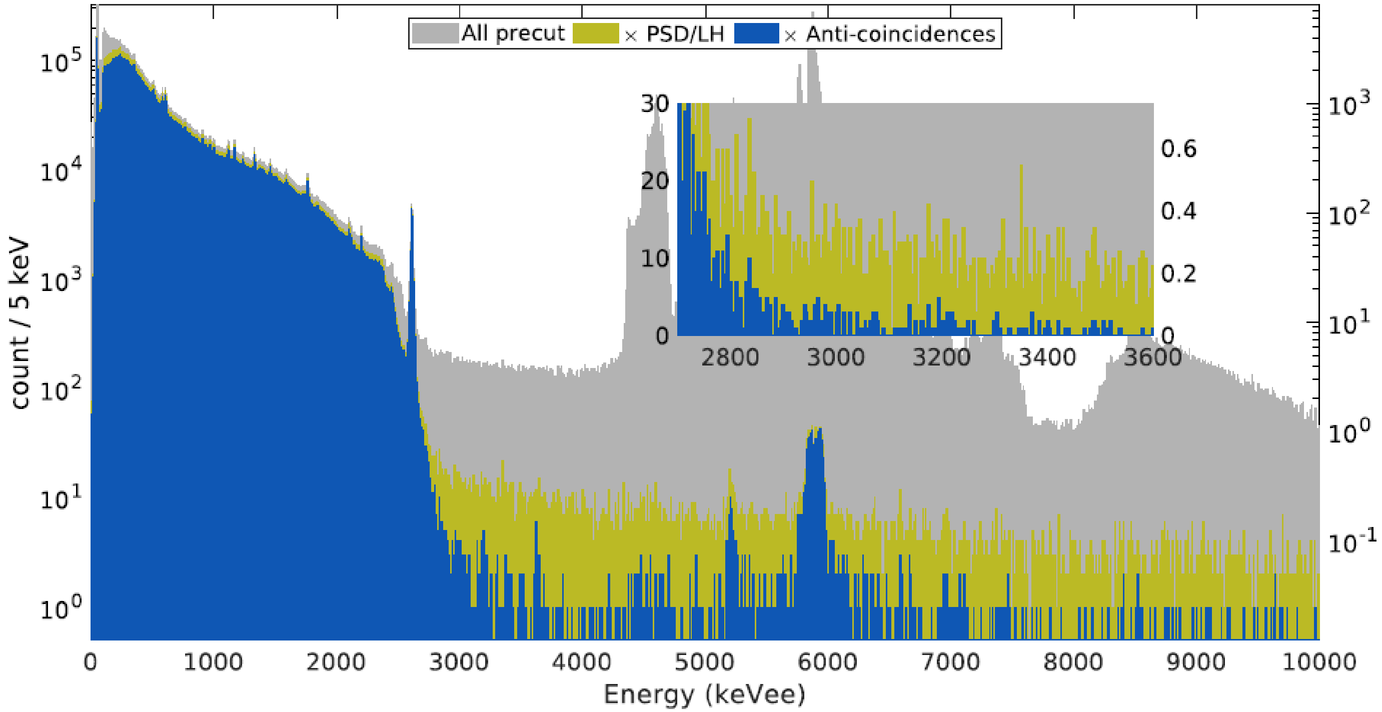

Live exposure	Bkg. @ $Q_{\beta\beta}$ / ckky
Total (8.02 kg_{XMoO_4} yr)	0.040±0.004
CMO (6.19 kg_{XMoO_4} yr)	0.039±0.004
LMO (1.83 kg_{XMoO_4} yr)	0.045±0.009

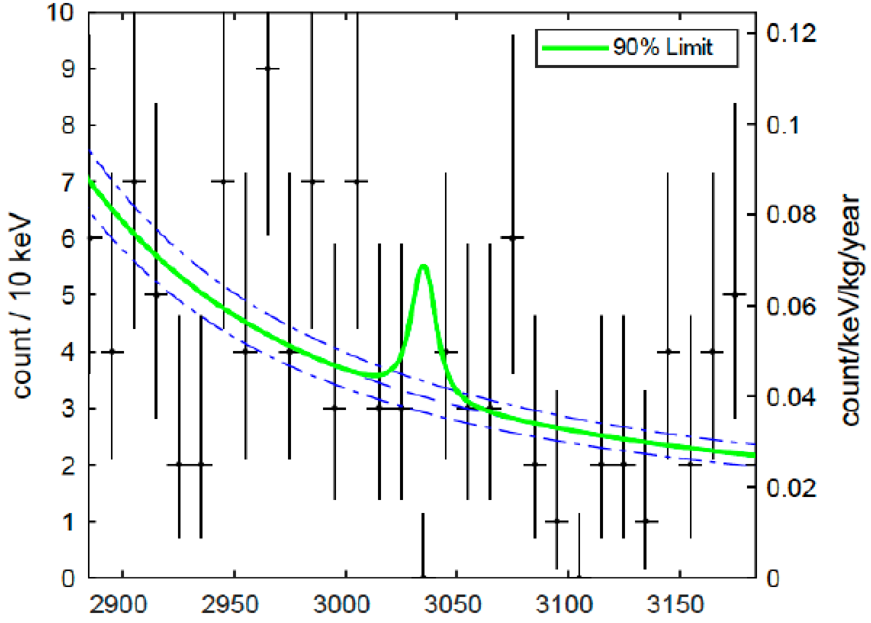

- 17 crystals excluding one LMO (for very poor β/α discrimination power)

  Exposure = 8.02 kgXMoO4 ・ yr = 3.88 kg100Mo ・ yr.

CMO has higher alpha backgrounds and rejection power is high

LMO has lower alpha backgrounds and rejection power is low

^{100}Mo 0νββ limit from AMoRE-I: $T_{1/2}^{0\nu\beta\beta} > 3{,}4 \times 10^{24}$ *years*

Current best limit 1.8×10^{24} *years* by CUPID-Mo

Yeongduk Kim (CUP IBS)
NPB 2024, Hong Kong

Limits & Sensitivities

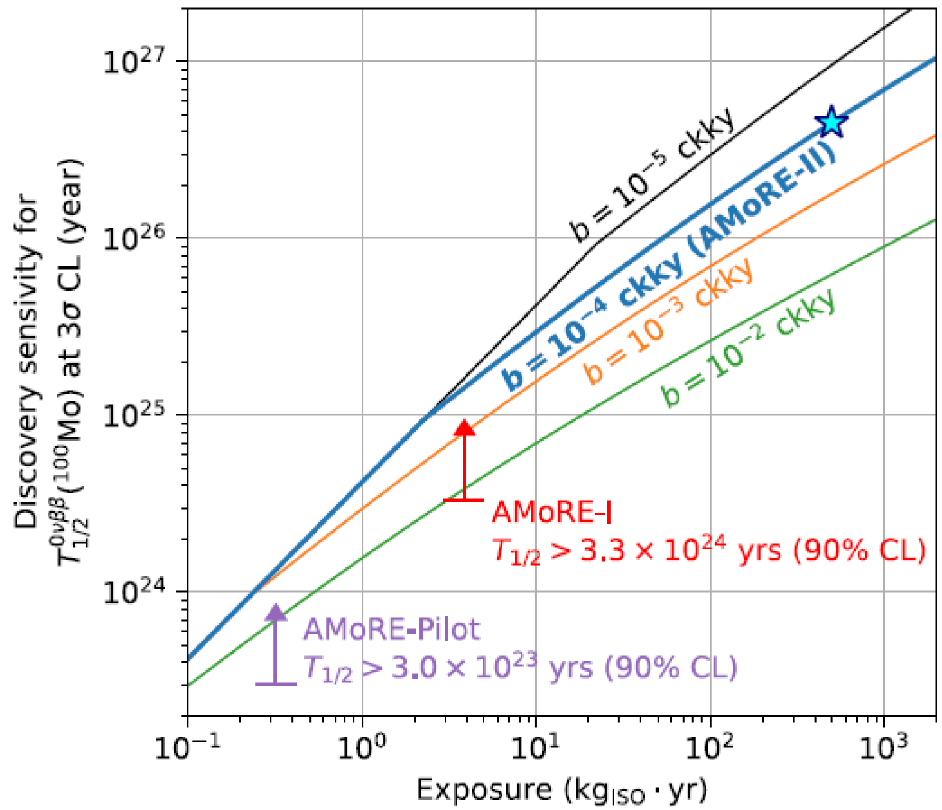

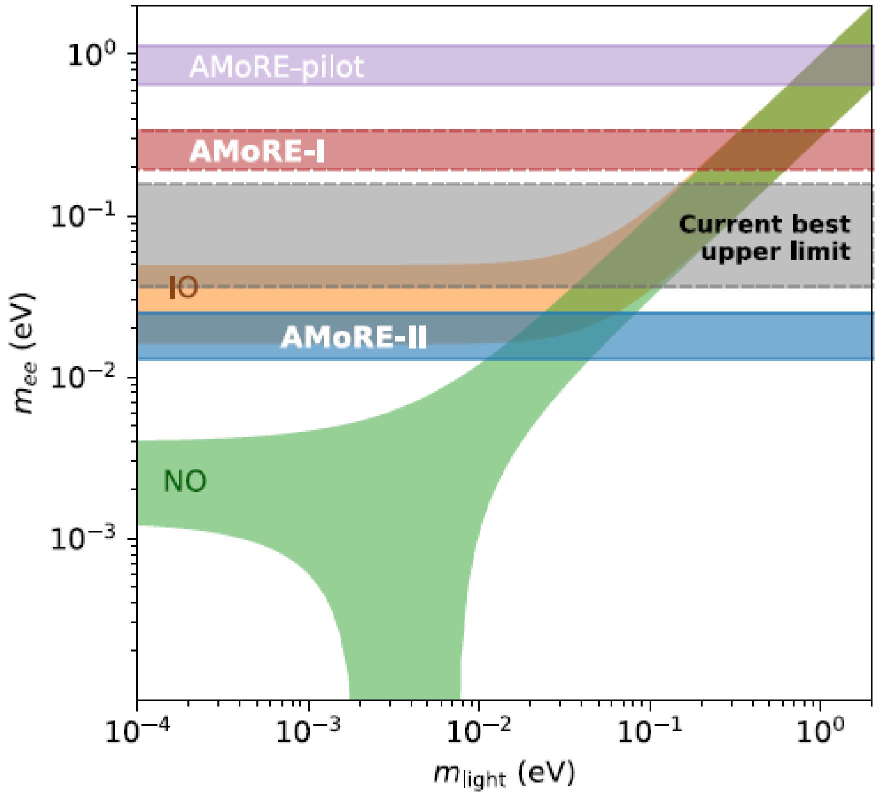

(By KamLAND-Zen Phys. Rev. Lett. 130 (2023) 051801)

- AMoRE-I result corresponds to $m_{\beta\beta}$<200-340 meV
- AMoRE-II for $T_{1/2}^{0\nu\beta\beta} > 5 \times 10^{26}$ years by 100 kg of ^{100}Mo × 5 years running.

Yoomin Oh (CUP IBS)
Neutrino 2022, Seoul

Underground Laboratories of the BNO INR RAS

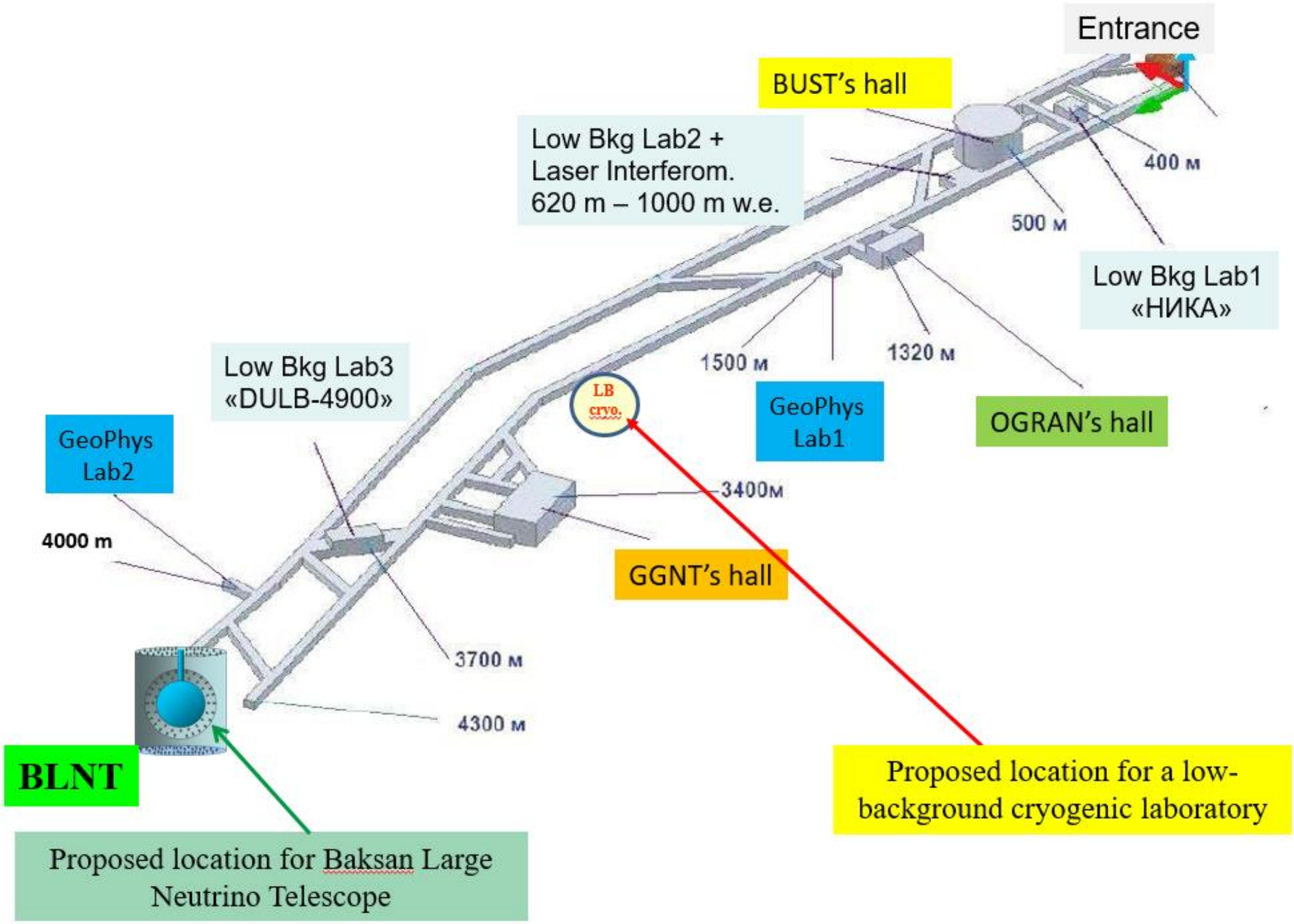

Cryogenic experiments

Two options for the development of cryogenic experiments at the BNO INR RAS are considered:

1) Liquefied noble gas detectors - xenon, argon.
2) Detectors based on scintillation crystals cooled to a temperature of 10 mK operating in the bolometer mode.

Liquefied noble gases (large sensing volume, easy to scale)

Two-Phase Emission Detector:

search for dark matter, search for axions, coherent elastic neutrino-nucleus scattering, detection of solar neutrinos (pp, 8B), SN-neutrinos

Bolometers (high energy resolution and registration efficiency)

study of $0\nu\beta\beta$ - decay of isotopes ^{100}Mo, ^{130}Te, ^{48}Ca, ^{82}Se, ^{116}Cd, ^{124}Sn
search for dark matter, axions
study of CEνNS
X-ray - spectroscopy

Thank you for your attention!

Backup slides

Angular distribution of total muons flux at GGNT laboratory (π-meson mechanism of muons generation

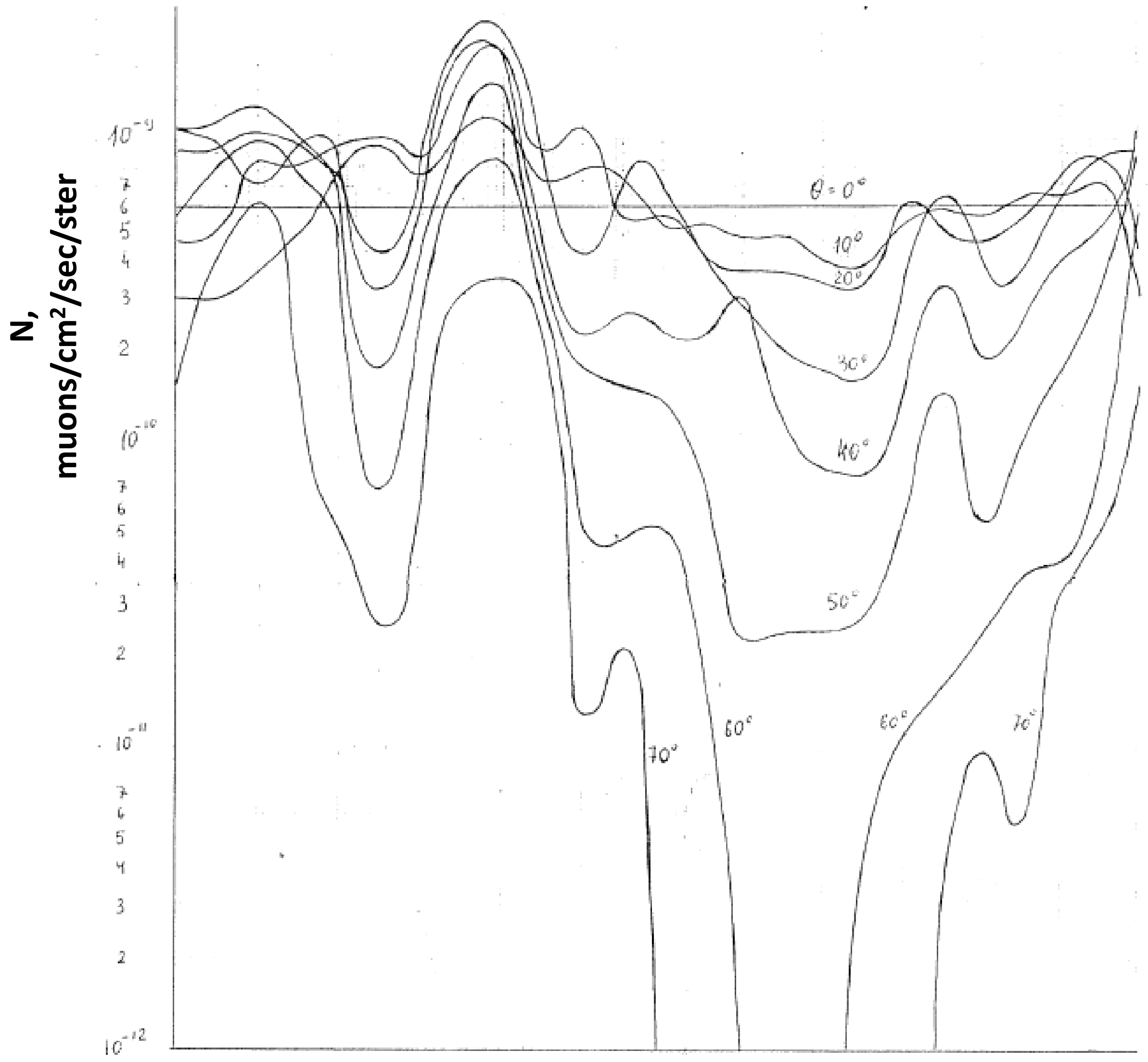

Characteristics of Baksan rock (shale)

Element	SiO_2	TiO_2	Al_2O_3	Fe_2O_3	FeO	MgO	CaO	Na_2O	K_2O	H_2O	CO_2	SO_3
Content, %	65,73	0,35	13,35	3,68	4,5	2,3	2,52	0,79	3,28	1,7	0,85	0,6

	238U	232Th	40K
Content, g/g	**$(1{,}5 \div 3{,}3) \cdot 10^{-6}$**	**$(1{,}9 \div 2{,}5) \cdot 10^{-5}$**	**$3{,}4 \cdot 10^{-6}$**
Gamma-activity of the rock, gamma/sec/gr	3,17E+4	1,17E+4	3,25 (natural)
	~ 0,47		
Unscattered gamma-flux	3,94 gamma/cm^2/sec $3{,}4 \cdot 10^5$ gamma/cm^2/day		

Neutron activity: $21{,}2 \cdot 10^{-3}$ neutrons/gr/day

Radon: ~ 10^{-12} Ci/L

Characteristics of Low background concrete based on dunite, quartz sand and selected Portland cement

Composition	Mass content, %	^{238}U, g/g	^{232}Th, g/g	^{40}K, g/g
Dunite crushed stone/rock (5÷20 mm)	1115 kg (48,5%)	< $3*10^{-9}$	$2,5*10^{-8}$	$7,7*10^{-9}$
Quartz sand (white inwash)	665 kg (28%)	$9,5*10^{-8}$	$4,0*10^{-7}$	$2,2*10^{-9}$
Portland cement (M-400)	370 kg (15,5%)	$1,5*10^{-6}$	$2,7*10^{-6}$	$1,33*10^{-7}$
Water	189 kg (8%)			
Sulfite waste liquor	additive	< $3,1*10^{-8}$	< $1,3*10^{-8}$	-
Plasticizing agent	additive	< $6,5*10^{-9}$	< $3,1*10^{-8}$	-

Neutron activity: $0,64*10^{-3}$ neutrons/gr/day

Примеры областей допустимых параметров (Δm^2, $\sin^2 2\theta$), полученных в BEST-2

Осцилляции подтверждаются, параметры определяются

Осцилляции подтверждаются, параметры не определяются

Есть зависимость от энергии нейтрино;
ГА объясняется не осцилляциями

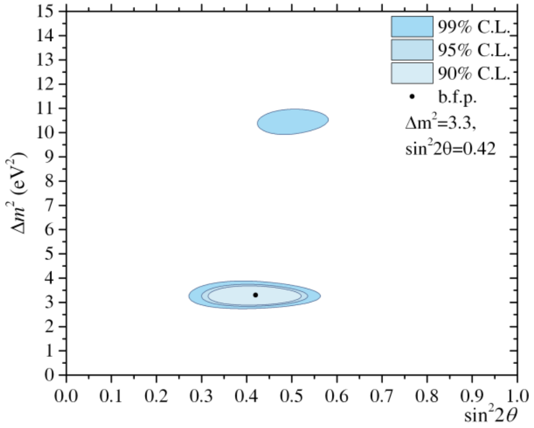

(Δm^2, $\sin^2 2\theta$) = (3.3 эВ^2, 0.42)

(R_1, R_2, R_3) = (0.70, 0.78, 0.94)

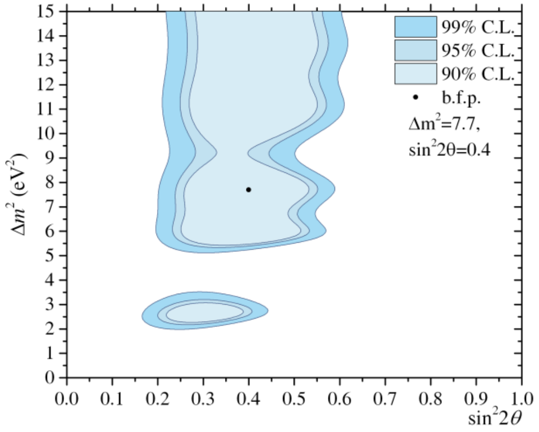

(7.7 эВ^2, 0.4)

(0.79, 0.77, 0.83)

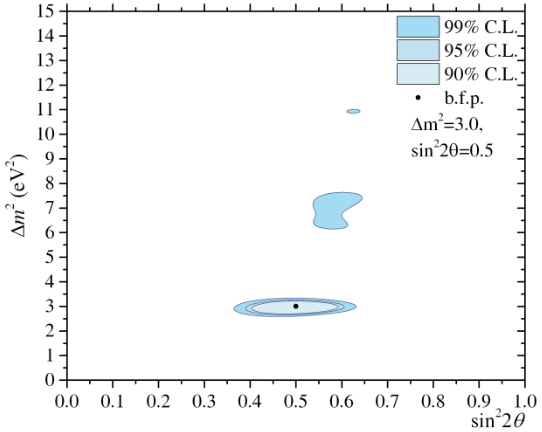

(3.0 эВ^2, 0.5)

(0.67, 0.65, 0.90)

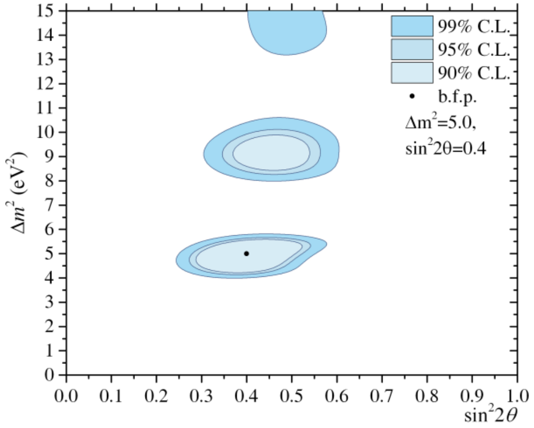

(5.0 эВ^2, 0.4)

(0.74, 0.89, 0.71)

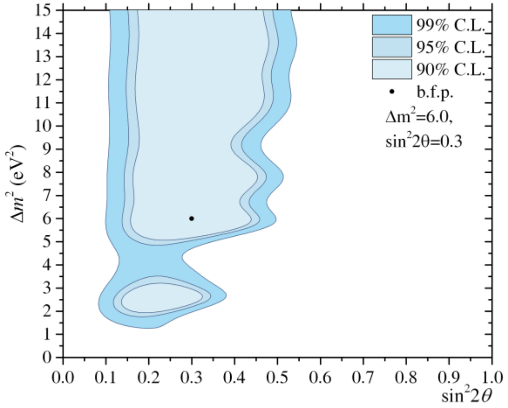

(6.0 эВ^2, 0.3)

(0.84, 0.82, 0.85)

YangYang Underground Laboratory (Y2L)

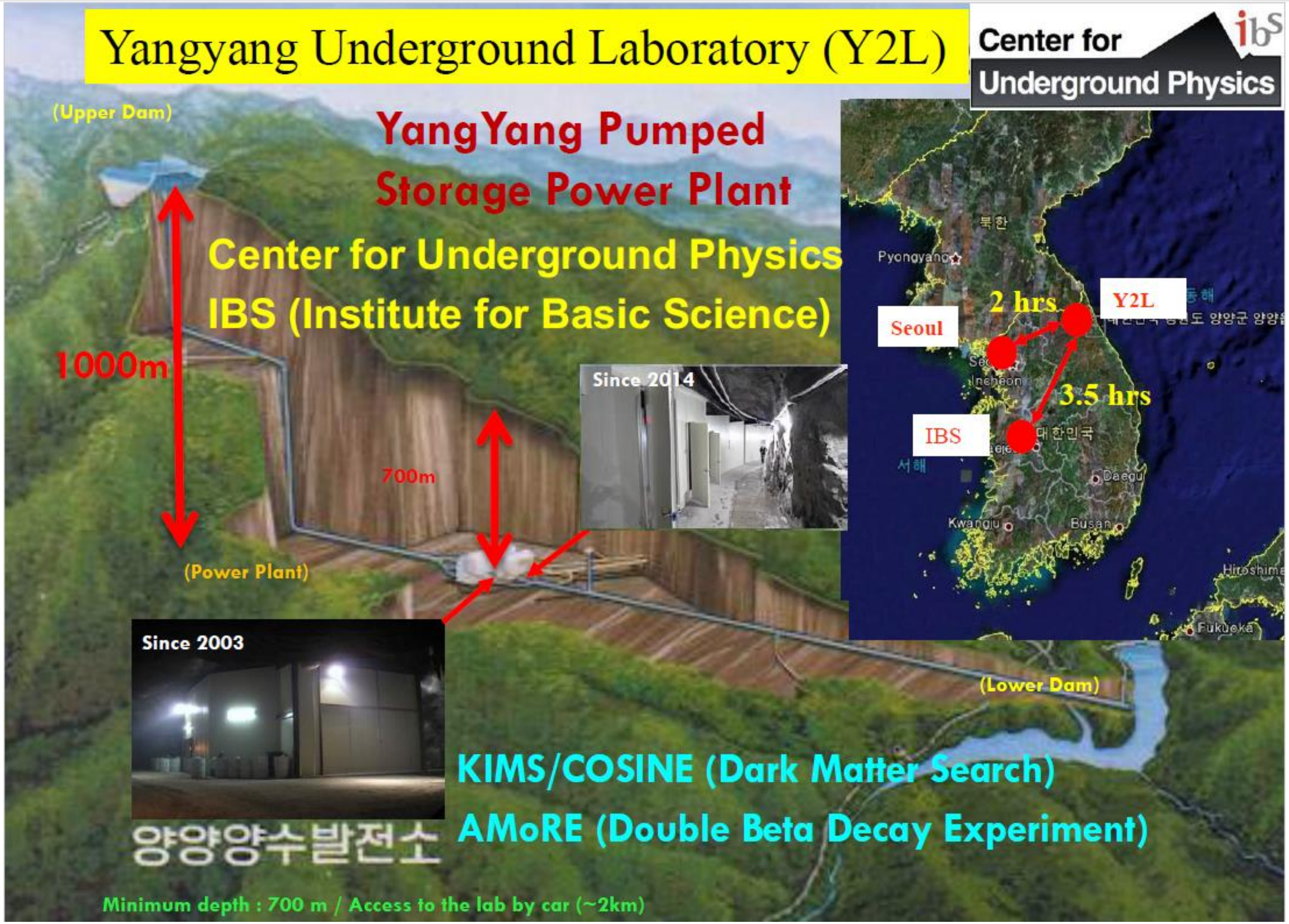

AMoRE-II @Yemilab

- Yemilab is constructed in 2022. (1000m deep)
- Lab space > 3000 m², 2.5 MW electricity.
- Two access ways: ramp-way, men-riding cage
- Open to other researchers IBS.

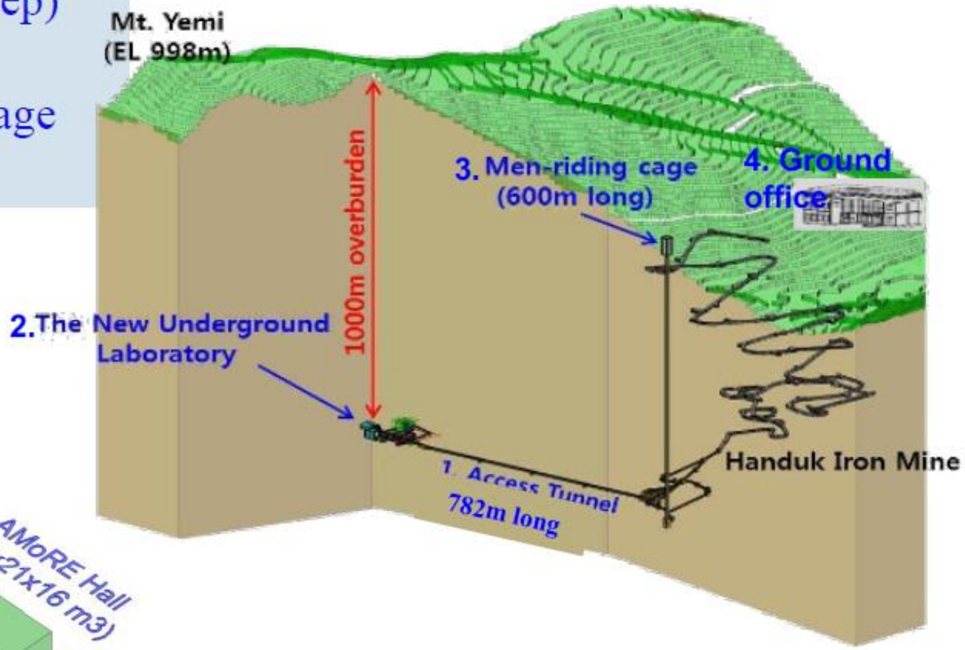

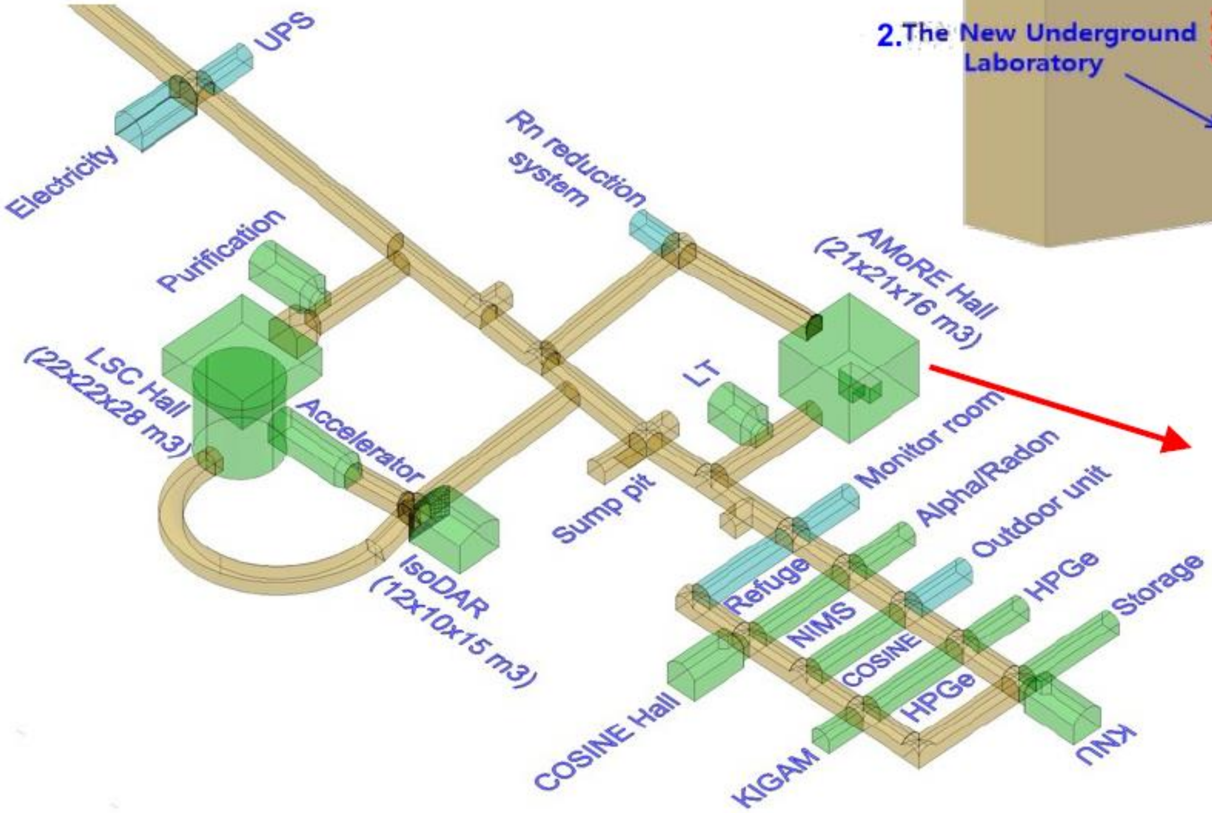

AMoRE-II detector

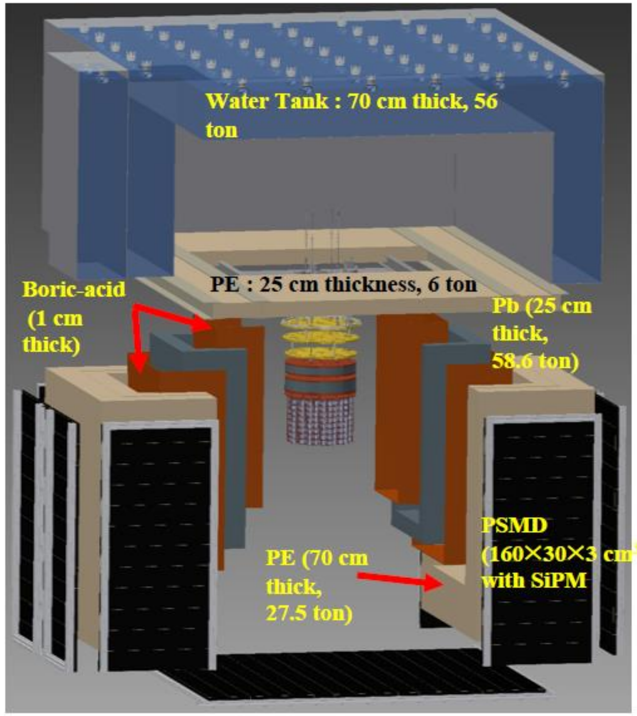

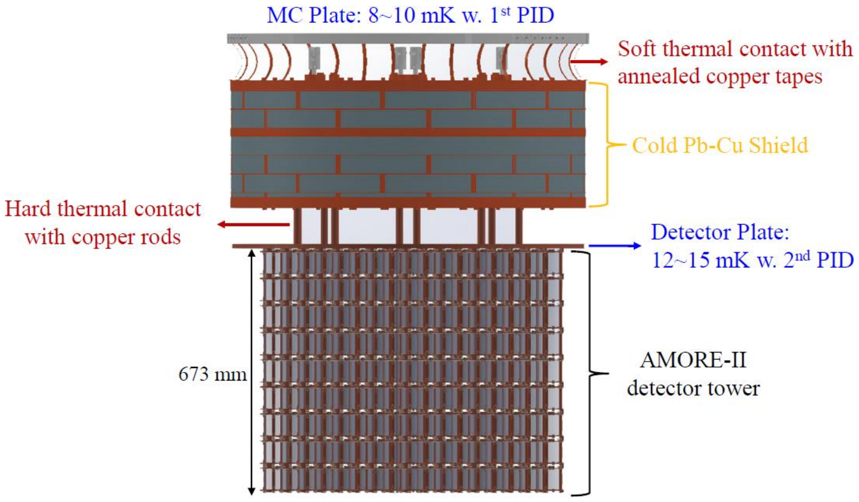

Preliminary

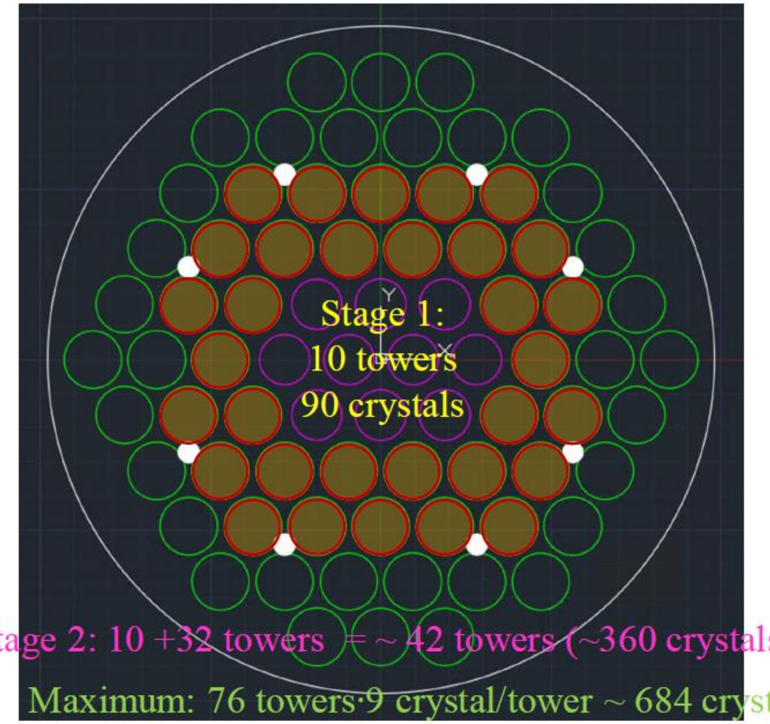

Stage 2: 10 +32 towers = ~ 42 towers (~360 crystals)

Maximum: 76 towers·9 crystal/tower ~ 684 crystals

Ultimate maximum: 50+26 towers·12 crystal/tower ~ 912 crystals

- The module designs are done for 5-cm and 6-cm LMOs.

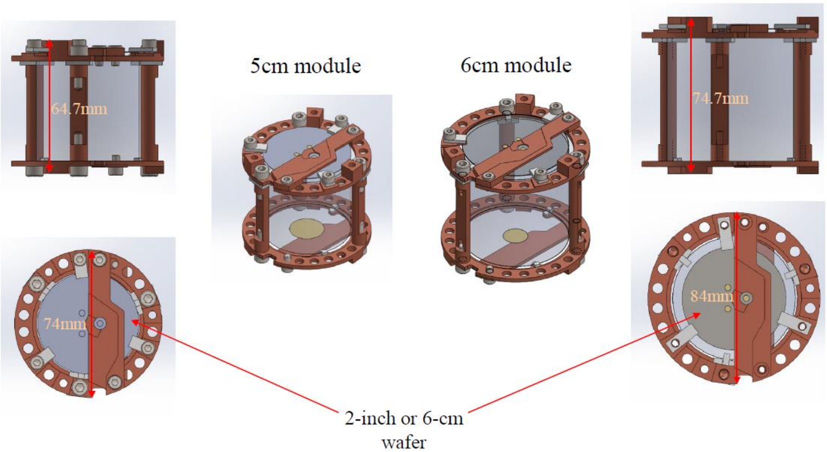

- LMO crystals: ∅5cm x H.5cm (310g) and ∅6cm x H.6cm (520g)
- Mass: ~80kg ^{100}Mo (~150kg crystal mass w. ~ 400 LMO crystals)

First Phase: 9 x10 ~ 24kg crystal mass

RESULTS

The total number of Kr-81 K-captures can be estimated from the area under the 13.5 keV TAP curve for all types of events as $N_K = N_K^{exp}/\varepsilon_d = 7.8 \times 10^6$, where $N_K^{exp} = 6.7 \times 10^6$ - the number of events with the energy of the region 13.5 ± 3.0 keV for a total of 1,175 live days of measurement; $\varepsilon_d = 0.869$ is the absolute efficiency to detect respective radiation.

$$N_{KK} = N_K \boxed{P_{KK}} \omega_{2K}\delta_e\eta = 57 \pm 8, \text{ where}$$

Events selection parameters

Kr-81

A_2~A_2~12 keV, 0.6<A_1<8.5 keV

$[K_\alpha^h \otimes K_\alpha^S \otimes (eA + e_K^{SO})]$

Kr-78

A_2~A_2~12 keV, 1<A_1<4 keV

$[K_\alpha^h \otimes K_\alpha^S \otimes eA]$

$N_K = 7.8 \times 10^6$ - the number of K-capture during 81 Kr decays.

$P_{KK} = 6.5 \times 10^{-5}$ - the probability of the double K-shell vacancy production per K-electron capture for Br-81. (Theoretical calculations)

$\delta_e = 0.6$ - the fraction of all ejected K-electrons registered in the coincidence according to the selection criteria.

$\eta = \varepsilon_p \cdot \varepsilon_3 \cdot \alpha_k$ with parameters:

$\varepsilon_p = 0.81 \pm 0.01$ - the probability of two K photons to be absorbed in the operating volume;

$\varepsilon_3 = 0.54 \pm 0.05$ - the efficiency to select three-point events;

$\alpha_k = 0.985 \pm 0.005$ - the fraction of events with two K photons that could be registered as distinct three-point events.

$$N_{coinc}^{dipl} = 42 \pm 6 \Rightarrow \boxed{P_{KK}^{SO}} = [5.7 \pm 0.8(stat) \pm 0.4(syst)] \times 10^{-5}$$

$$N_{coin}^{enr} = 16 \pm 4 \qquad T_{1/2}^{2\nu 2K} = \ln 2 * N_A \times \frac{p_3 * \varepsilon_f * t}{N_{coin}^{enr}} = [1.9^{+1.3}_{-0.7}(stat) \pm 0.3(syst)] \times 10^{22} \text{ yr}$$

$N = 1.08 \cdot 10^{24}$ - the number of Kr-78 atoms in the fiducial volume of the counter

$p_3 = 0.47$ - the fraction of 2K-captures accompanied by the emission of two K-photons.

The efficiency is calculated as $\varepsilon_f = \varepsilon_p \cdot \varepsilon_3 \cdot \alpha_k \cdot k_\lambda$,

$k_\lambda = 0.85$ - the useful event selection coefficient for a given threshold for λ

$t = 787.7$ days of live measurement

Double K-Vacancy Production in Xenon by 88-keV Gamma-ray Photoionization

Such a rare phenomenon as a double-K-shell photoionization of the atom can create the "hollow atom" by absorbing a single photon and releasing both K-electrons. Detection of such a process is possible by observing double-K-satellite fluorescence transitions during relaxation of these states. This process can be a source of background in an experiment to search for 2K-capture of ^{78}Kr,^{124,126}Xe and, at the same time, serve as a methodological test for analyzing the accumulated data.

Comparative study of the double-K-shell-vacancy production in single- and double-electron-capture decay,

https://doi.org/10.1103/PhysRevC.96.065502

K and L shell emission lines in electron volts

Kr Kα1 = 12649; Kα2 = 12598; Kβ1 = 14112 eV
Xe Kα1 = 29779; Kα2 = 29458; Kβ1 = 33624 eV

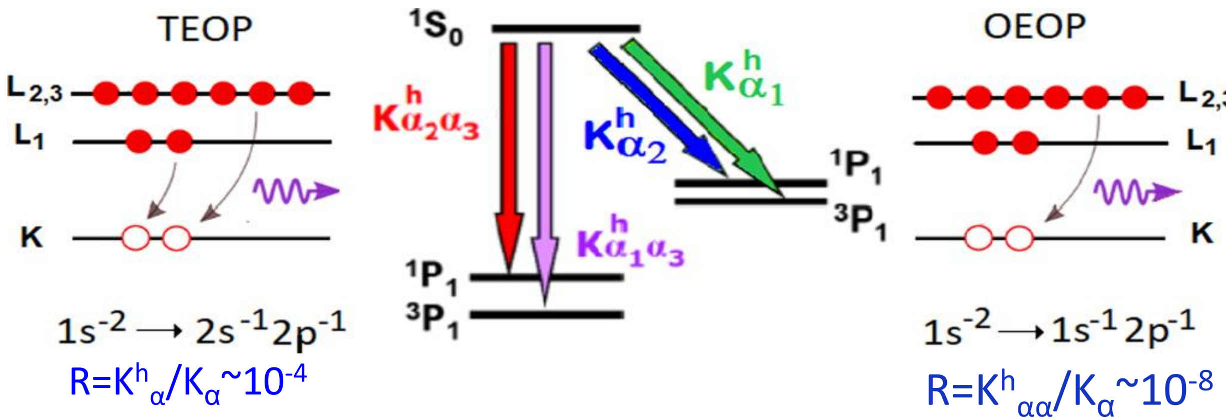

Schematic of the two electron one-photon (TEOP) or one-electron one-photon (OEOP) transitions and the atomic-level-decay diagram for the initial K-shell. The first fluorescence quantum $K^h\alpha_1$ differs most from the energy of $K\alpha_1$, with the energy difference being equal to ~360 and ~680 eV for Kr and Xe, respectively.

Detector response to simultaneous registration of two X-ray photons and an Auger electron

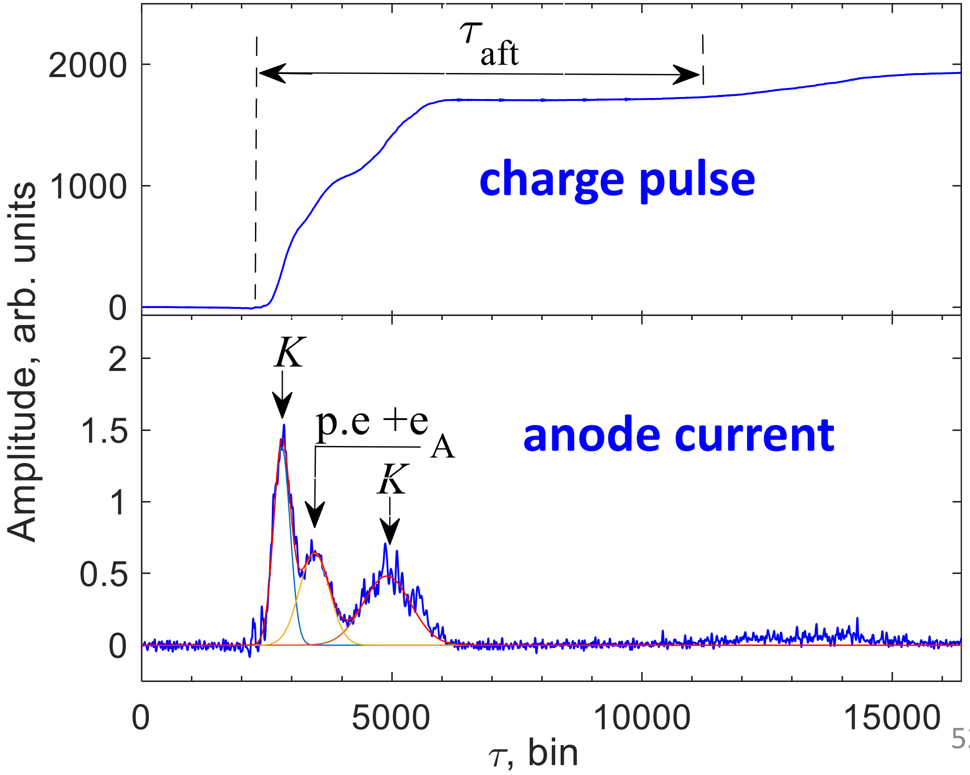

Solar axions spectra vs $g_{A\gamma}$, g_{Ae} and g_{AN}

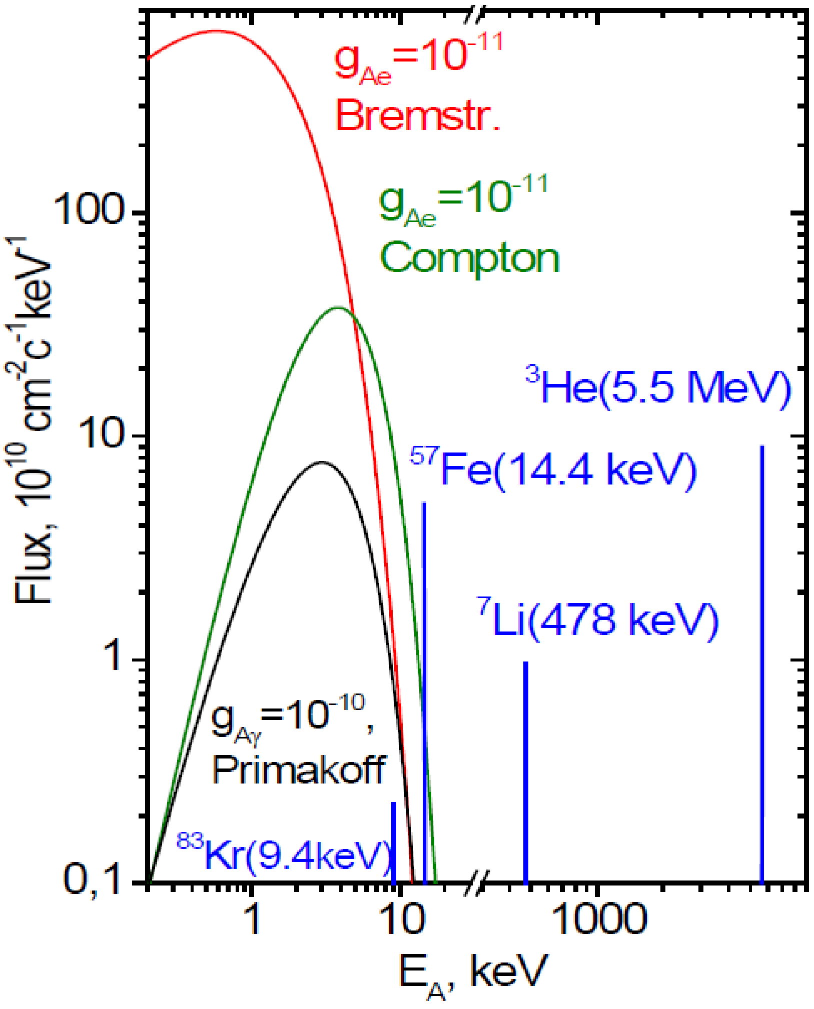

The main mechanisms of appearing of solar axions:

1. Reactions of main solar chain. The most intensive fluxes are expected from M1-transitions in ^{7}Li and ^{3}He nuclei(g_{AN}):
$^7Be+e^- \rightarrow Li^*+\gamma$; $^7Li^* \rightarrow {}^7Li+A$(478кэВ)
$p + d \rightarrow {}^3He + A$ (5.5 МэВ).
2. Magnetic type transitions in nuclei whose low-lying levels are excited due to high temperature in the Sun (^{57}Fe, ^{83}Kr)(g_{AN})
3. Primakoff conversion of photons in the electric field of solar plasma($g_{A\gamma}$).
4. Bremsstrahlung: $e+Z(e) \rightarrow Z+A$.(g_{Ae})
5. Compton process :$\gamma+e \rightarrow e+A$.(g_{Ae})
6. axio-recombination: $e + I \rightarrow I^- + A$ and axio-deexcitation: $I^* \rightarrow I + A$.

PRD 83 023505 (2011) CAST 1302.6283, 1310.0823

Flux of solar axions from ^{83}Kr

The total axions flux Φ_A depends on the nuclear excitation level E_γ =9.4keV, temperature of the Sun media T, nuclear level lifetime τ_γ=3.6μs, abundance of the ^{83}Kr isotope on the Sun N, and the branching ratio of axion to photon emission ω_A/ω_γ:

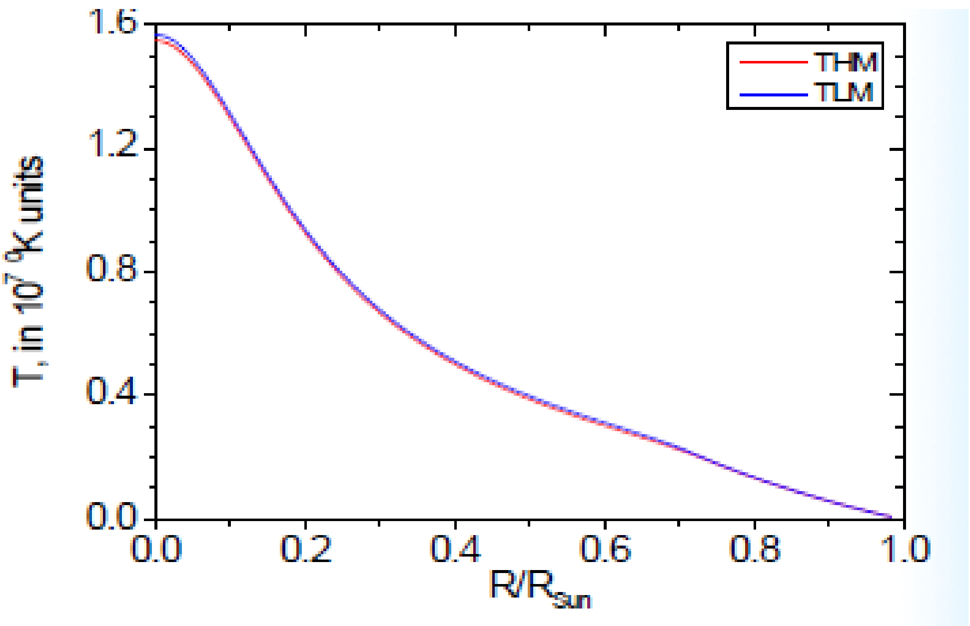

$$\Phi_A = \int N(r) \frac{2\exp(-E_\gamma / kT(r))}{1+2\exp(-E_\gamma / kT(r))} \frac{\omega_A}{\tau_\gamma \omega_\gamma} dr$$

$$\Phi_A(E_{M1}) = 5.97\times 10^{23} \left(\frac{\omega_A}{\omega_\gamma}\right) \mathrm{cm^{-2}s^{-1}keV^{-1}}$$

$$m_a = \frac{\sqrt{z}}{1+z}\frac{f_\pi m_\pi}{f_a} = 1\mathrm{eV}\,\frac{\sqrt{z}}{1+z}\frac{1.3\cdot 10^7}{f_a/GeV}$$

where m_π и f_π – mass and decay constant of neutral pion, $z=m_u/m_d=0.56$ – quark mass ratio ($f_\pi \approx$ 93 MeV).